SMART 2021

The Tenth International Conference on Smart Systems, Devices and Technologies

ISBN: 978-1-61208-863-1

May 30th – June 3rd, 2021

SMART 2021 Editors

Lasse Berntzen, University of South-Eastern Norway, Norway

Sergio Ilarri, University of Zaragoza, Spain

Oana Dini, IARIA, EU/USA

SMART 2021

Foreword

The Tenth International Conference on Smart Systems, Devices and Technologies (SMART 2021), held between May 30 – June 3rd, 2021, continues a series of events covering tendencies towards future smart cities, specialized technologies and devices, environmental sensing, energy optimization, pollution control and socio-cultural aspects.

Digital societies take rapid developments toward smart environments. More and more social services are digitally available to citizens. The concept of 'smart cities' including all devices, services, technologies and applications associated with the concept sees a large adoption. Ubiquity and mobility added new dimensions to smart environments. Adoption of smartphones and digital finder maps, and increasing budgets for technical support of services to citizens settled a new behavioral paradigm of city inhabitants.

We take here the opportunity to warmly thank all the members of the SMART 2021 Technical Program Committee, as well as the numerous reviewers. The creation of such a broad and high quality conference program would not have been possible without their involvement. We also kindly thank all the authors who dedicated much of their time and efforts to contribute to SMART 2021. We truly believe that, thanks to all these efforts, the final conference program consisted of top quality contributions.

Also, this event could not have been a reality without the support of many individuals, organizations, and sponsors. We are grateful to the members of the SMART 2021 organizing committee for their help in handling the logistics and for their work to make this professional meeting a success.

We hope that SMART 2021 was a successful international forum for the exchange of ideas and results between academia and industry and for the promotion of progress in the field of smart systems, devices and technologies.

SMART 2021 Chairs:

SMART 2021 Steering Committee
Lasse Berntzen**,** University of South-Eastern Norway**,** Norway
Young-Joo Suh, POSTECH, Korea

SMART 2021 Publicity Chair
Marta Botella-Campos, Universitat Politecnica de Valencia, Spain
Daniel Basterretxea, Universitat Politecnica de Valencia, Spain

SMART 2021

COMMITTEE

SMART 2021 Steering Committee

Lasse Berntzen**,** University of South-Eastern Norway**,** Norway
Young-Joo Suh, POSTECH, Korea

SMART 2021 Publicity Chairs

Marta Botella-Campos, Universitat Politecnica de Valencia, Spain
Daniel Basterretxea, Universitat Politecnica de Valencia, Spain

SMART 2021 Technical Program Committee

Lounis Adouane, Université de Technologie de Compiègne / Heudisayc, France
Ramakalyan Ayyagari, National Institute of Technology Tiruchirappalli, India
Karolina Baras, University of Madeira, Portugal
Lasse Berntzen, University of South-Eastern Norway, Norway
DeJiu Chen, KTH Royal Institute of Technology, Sweden
Patrizio Dazzi, ISTI-CNR, Italy
María del Mar Gómez Zamora, Universidad Rey Juan Carlos, Spain
Marta Sylvia del Río, Universidad de Monterrey, Mexico
Rachid El Bachtiri, USMBA University, Morocco
Steffen Fries, Siemens AG, Germany
Marco Furini, University of Modena and Reggio Emilia, Italy
Angelo Furno, LICIT laboratory - University of Gustave Eiffel / University of Lyon, France
Ivan Ganchev, University of Limerick, Ireland / University of Plovdiv "Paisii Hilendarski", Bulgaria
Maria Helena Gomes de Almeida Gonçalves Nadais, University of Aveiro, Portugal
Jorge J. Gomez-Sanz, Universidad Complutense de Madrid, Spain
Javier Gozalvez, Universidad Miguel Hernandez de Elche, Spain
Somak Datta Gupta, Ford Motor Company, USA
Fakhrul Hazman Yusoff, Universiti Teknologi MARA, Malaysia
Gerold Hölzl, University of Passau, Germany
Tzung-Pei Hong, National University of Kaohsiung, Taiwan
Javier Ibanez-Guzman, Renault, France
Sergio Ilarri, University of Zaragoza, Spain
Abdelmajid Khelil, Landshut University of Applied Sciences, Germany
Pinar Kirci, Bursa Uludag University, Turkey
Kirill Krinkin, Saint-Petersburg Electrotechnical University, Russia
Wolfgang Leister, Norsk Regnesentral, Norway
Giovanni Livraga, Universita' degli Studi di Milano, Italy
Giuseppe Mangioni, University of Catania, Italy
Manuel Mastrofini, Università degli studi di Roma Tor Vergata & LAST Horizon, Italy
Natarajan Meghanathan, Jackson State University, USA
Dmitry Namiot, Lomonosov Moscow State University, Russia

Copyright Information

For your reference, this is the text governing the copyright release for material published by IARIA.

The copyright release is a transfer of publication rights, which allows IARIA and its partners to drive the dissemination of the published material. This allows IARIA to give articles increased visibility via distribution, inclusion in libraries, and arrangements for submission to indexes.

I, the undersigned, declare that the article is original, and that I represent the authors of this article in the copyright release matters. If this work has been done as work-for-hire, I have obtained all necessary clearances to execute a copyright release. I hereby irrevocably transfer exclusive copyright for this material to IARIA. I give IARIA permission or reproduce the work in any media format such as, but not limited to, print, digital, or electronic. I give IARIA permission to distribute the materials without restriction to any institutions or individuals. I give IARIA permission to submit the work for inclusion in article repositories as IARIA sees fit.

I, the undersigned, declare that to the best of my knowledge, the article is does not contain libelous or otherwise unlawful contents or invading the right of privacy or infringing on a proprietary right.

Following the copyright release, any circulated version of the article must bear the copyright notice and any header and footer information that IARIA applies to the published article.

IARIA grants royalty-free permission to the authors to disseminate the work, under the above provisions, for any academic, commercial, or industrial use. IARIA grants royalty-free permission to any individuals or institutions to make the article available electronically, online, or in print.

IARIA acknowledges that rights to any algorithm, process, procedure, apparatus, or articles of manufacture remain with the authors and their employers.

I, the undersigned, understand that IARIA will not be liable, in contract, tort (including, without limitation, negligence), pre-contract or other representations (other than fraudulent misrepresentations) or otherwise in connection with the publication of my work.

Exception to the above is made for work-for-hire performed while employed by the government. In that case, copyright to the material remains with the said government. The rightful owners (authors and government entity) grant unlimited and unrestricted permission to IARIA, IARIA's contractors, and IARIA's partners to further distribute the work.

Table of Contents

Enhancing Spatial Image Datasets For Utilisation in A Simulator for Smart City Transport Navigation

Lepekola I. Lenkoe
Department of Electrical, Electronic and Computer Engineering
Central University of Technology, Free-State
Bloemfontein, South Africa
e-mail: pexonl3@gmail.com

Ben Kotze)
Department of Electrical, Electronic and Computer Engineering
Central University of Technology, Free-State
Bloemfontein, South Africa
e-mail: bkotze@cut.ac.za

***Abstract*—The introduction of Google Street Views has brought to surface a method for roof-mounted mobile cameras on vehicles. This method is regarded as one of the highly known and adopted methodologies for capturing street-level images. This article contributes to the development and implementation of Image-Based Rendering techniques by presenting a technique utilising a hexagon-based camera configuration model for image capturing. Upon the image capture stage, each segment camera is stored in a specific folder relative to the camera number (i.e., camera 1 = folder 1). Subsequently, the optimal image rendering process of each image blending takes place inside Blender3D software where image datasets are rendered for utilisation in a simulator. Utilising the Structure of Motion algorithm, dense point image, and its features, match detection is obtained. This article further contributes to the results process that allows for free movement within a 3D rendered scene by permitting for back and forward movement as compared to a slide show that only permits for forwarding motion.**

Keywords-Image-Based Rendering; Blender3D; Simulation; Datasets; Google Street Views; Smart Cities.

I. INTRODUCTION

Over the years, different kinds of techniques have been proposed for image data collection and image rendering. In the past few years, the Image-Based Rendering (IBR) technique has gained a lot of attention mainly in the image processing, computer vision, and computer graphics community. In addition to IBR's interest in communities, spatial knowledge which is regarded as an essential subject that makes use of geospatial statistics such as geoscience, geography has shown growth with regards to multi-functional ecosystems.

The street views have debilitated previous restrictions on the availability of data sources for evaluating streets [1][2]. Furthermore, Model-Based Rendering (MBR) is classified as an easy method for reconstructing virtual view from any arbitrary viewpoint by using explicit 3D geometric and model and texture information about the scene, while IBR is a method that constructs virtual view by using several images captured beforehand [3].

The captured images can provide valuable information about the incident, e.g., location. The location has the exact Global Positioning System (GPS) coordinates, which can also be an estimation of the location. Figure 1 presents the graphical representation of inquiring a query image to the reference database to find the match between a stored image and the query image [4].

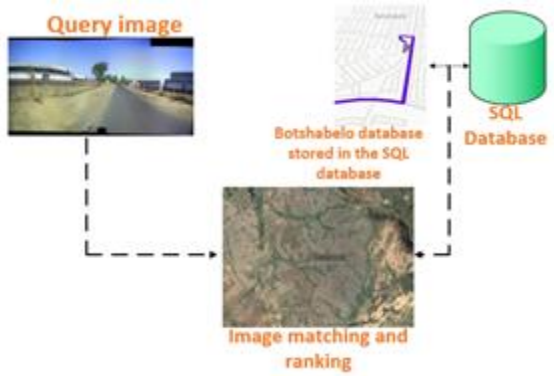

Figure 1. Street-view to overhead view image matching.

This article seeks to develop a 3D rendered model from a 2D captured model and allow for back and forward motion within a simulator. The 3D data acquisition process provides the probe position and orientation that remain in static order to produce accurate datasets. A single 3D capacity is not able to support the translational motion of the simulated probes, thus the need to develop a methodology for recording and capturing single 2D images and amalgamating the images into multiple 3D images within a single unit. Furthermore, the issue of emulating street-view images for multiple image transitions for application in geolocalisation for utilisation in a simulator needs to be investigated.

This paper is structured as follows: Section II describes the aim and objectives, and also outlines the contributions of this research. Additionally, Section III gives a brief description of the work done in this field, while Section IV describes the process and the development of the proposed model from the captured data up to data simulation. Section V discusses the results obtained from this study, while Section VI discusses the conclusion of the study.

 ISBN: 978-1-61208-863-1

A. *The Objective of This Study Is Therefore To:*

- To identify datasets with capabilities such as frame position, frame elevation, and frame indexing.
- To incorporate the system into the simulation system in real-time for increasing the reality of the simulation system in different geographical locations.

B. *Original Contributions of This Research Article*

This research article has produced the following contribution in furthering the article the knowledge contribution in the field of computer vision as follows:

- 6 degree of freedom- where the user can move in any direction as opposed to the use of single slides show that allows for one-directional movement in a street view scene.
- The ability of the application to use multiple cameras between 3 to 6 inputs as opposed to the use of single omnidirectional camera feedback and still obtain the same output rendered panoramic and simulated results.

II. LITERATURE REVIEW

Quintessentially, massive amounts of image collections are presented as slideshows, which are arguably the practical way but with the current technological advancement, these methodological approaches are deemed not engaging. The change in scenery due to technological improvements has led to a wide study pool, which also cites the research conducted by Sivic et al. [5]. In that work, the authors highlight the connection of clustering visually similar images together to create a virtual space in which the users are free to change position from one image to another. This virtual space modelling can be obtained by utilising intuitive 3D control objects such as move left/right, zoom in/out and rotate. Sivic further supports his work by outlining that the displayed images in a correct geometric and photometric alignment concerning the current photo, results in a smooth transition between multiple images. In addition, Kopf et al. [6] present a method of combining images in the street view system by stitching the image side views. This approach means that standing on the street and looking in either the left or right direction of a certain street together to generate a long street slide for users to quickly browse this street is feasible.

Despite the excellent way of viewing the side scene of a certain street from Kopf`s methodology, however, the practicality of that method is not always the case while driving or walking. Kopf further presents the street slide methodology which combines the nature of bubbles provided by perspective stripe panoramas. Kopf further presents integrated annotations and a mini-map within the user interface to provide geographic information as well as the additional affordances for navigation.

Kopf`s work relates to Gortler et al. [7] due to their classic approaches of image-based rendering such as Lumigraph. Kopf's work is further supported by Agarwala et al. [8] by emphasising the utilising of the correlation alignment techniques for aligning adjacent vertical strips instead of modeling the full 3D geometric proxies. Subsequent to these approaches, rendering displacement in maps requires the surface to be adaptively retesselated [9].

The synthetic environments for the extraction of the depth information during the rendering process. The geometric construction relates to both implicit and explicit construction [10]. This is as a result of the view dependency, which means that the explicit geometric rendering much relies on the known approximate environment [11]. The use of the explicit rendering becomes much tricky in an informal environment/settlement due to the tiring exercise of data collection which is skewed since residents can build on the road and mountains.

III. METHODOLOGY

The simulator model design is developed for a driver or person riding a bicycle inside the simulator following a track in either forward or reverse direction. With this said, the initial thought design was to develop the Spatial Image Datasets (SID) based on the nonagon (9) camera configuration model. However, with the current technological capabilities, an omnidirectional camera could have been utilised to conduct this activity. The reason for not utilising the omnidirectional camera is because the rendering construction specifically for this research article requires individual camera feeds as opposed to one 360º feed. It is however, Yuah et al emphasized that the 6D object pose estimation is a challenging but important research direction in visual direction [12].

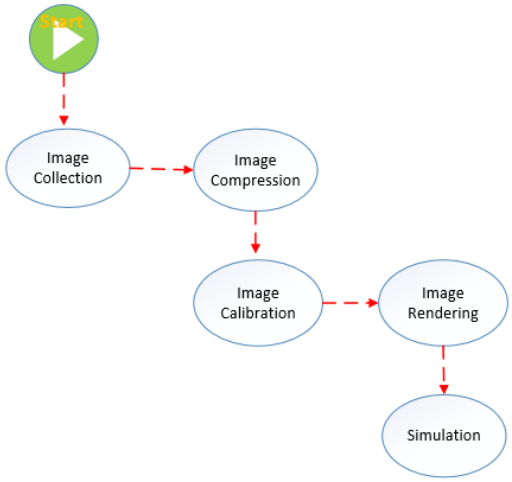

Figure 2. System model layout.

The system development was then initiated based on the model layout as indicated in Figure 2. Figure 2 depicts the technical approach for the design and development of the simulator utilising the hexagon camera configuration model.

Subsequently, Wang et al. [13] depict their method for integrating the IBR and NERF methods into s new learning method that generates a continuous multiple source view for rendering novel views. However, Wang's study does not clearly outline the dataset generation and the creation of

scenes from the dataset of an image that was not initially captured.

A. Image Capturing and Collection

The image capture section consists of the following apparatus; camera, images, and GPS coordinates. The six (6) mounted camera configuration model for image capture while the vehicle is in motion, and each image is treated as a frame. During the image capturing process, each camera image dataset is stored in its specific folder i.e., camera 1 = folder 1.

B. Image Compression

The scene depiction utilising multiple depth images in a dataset format is compressed. The image samples are then captured and obtained from the camera capture by delaying the camera switching algorithm between multiple cameras by 3ms (the delay period was based on the trial and error test conducted between 1ms – 5ms switching).

Furthermore, the Lossy compression algorithm is performed for the redundant processing of image information. Additionally, the image dataset is simulated without noise for better performance verification as outlined in Figure 3 utilising the Lossy compression algorithm.

Figure 3. image compression on a JPE file.

Figure 3 depicts the image types for the captured images. Subsequently showing the timestamp and the GPS coordinates for the image dataset created. Additionally, the image compression framework is used to obtain the results output outlined in Figure 4.

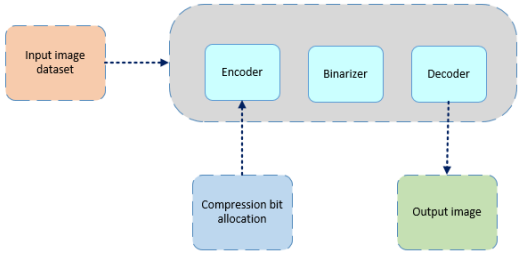

Figure 4. Compression structure.

Figure 4 depicts the compression structure that utilised the input image datasets for the network training sample. This is obtained by specifically setting the image dataset for image recognition where the compressed image datasets are compared against the raw image datasets. Additionally, the image compression bit allocation is then used to calculate the compression alterations. However, the alterations depend on the size of the dataset. Notably, each image in the dataset is compressed individual is to retain the image quality. However, this is deemed as a tedious process, especially for huge datasets.

C. Image Calibration

The data collection and image compression process, are determined by the reduction in the image size but still keeping the image resolutions intact. The image calibration model utilises the pinhole camera model that introduces some image distortions. These image distortions that are seen in this process are classified as radical image distortion. The radical image distortion was calculated as follows:

$$X_{distortion} = x(1 + k_1 r^2 + k_2 r^2 + k_3 r^6) \quad (1)$$

$$Y_{distortion} = y(1 + k_1 r^2 + k_2 r^2 + k_3 r^6) \quad (2)$$

Where: x = original; x location on the imager
y = original y location on the imager
k = radical distortion coefficient
r = radical distortion form Taylor series

The system setup approach makes use of the chess pattern for camera calibration setup. Some calibration methods in the literature rely on 3D objects. However, through the tests conducted, the flat chessboard pattern approach is deemed appropriate for this research article due to the method been less complex and easily understood even by non-technical individuals.

The camera calibration process is as follows:

- Capture 20 chessboard images from different poses;
- Find the chessboard corners;
- Find the intrinsic matrix, distortion coefficients, rotation vectors, and the translation vector;
- Store the .xml file.

Following the process completion, OpenCV for the python library is utilised to compute the results from the .xml file. This, therefore, allows for the reuse of the code for multiple cameras, which is relevant for this research paper which uses a hexagon camera configuration model with rotational image capture technique.

 ISBN: 978-1-61208-863-1

Figure 5. Black and white test match on a chessboard.

The black and white squared pattern match-finding is outlined as indicated in Figure 5 for the identification of features within a 2D image. The pattern match-finding is important in the extraction of image data from multiple image datasets that are the same.

D. Image Rendering Procedure

The image rendering technique in the context of this research article focuses on the known camera parameters and undistorted images for the rendering of the scenes. These images are reconstructed, and the texture is applied to their structure before rendering simulation can be executed.

E. Structure for Motion

The basic operation of the structure of motion in this research article follows the Detection of 2D features on every image. In this step, a 2D feature is detected using the Scale-Invariant Feature Transform (SIFT) algorithm as indicated in Figure 6. Figure 6 depicts the original image captured with one of the mounted cameras from the hexagon configuration model.

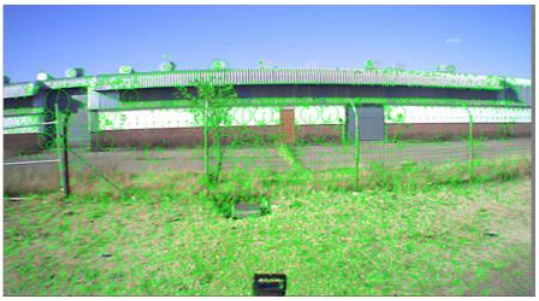

Figure 6. Detecting the image feature using SIFT.

The camera parameters are captured, and the patch-based stereo and semi-global matching are used to generate point tracks, depth-maps as well as the points cloud. Upon successful generation of these variables, a mesh of the scene is created as indicated in Figure 7. Finally, all the refined depth maps are merged to get the final reconstruction.

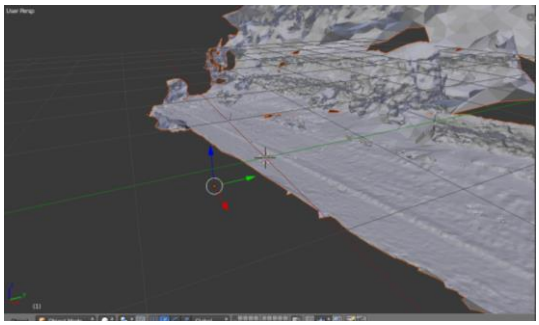

Figure 7. Mesh output from the multiview stereo.

The multi-view stereo algorithm is further used as a Semi-Global Matching algorithm (SGM), where it consists of calculation, aggregated costs, disparity computation, and the extension for multi-baseline matching.

F. Texturing

Patches are formed onto the faces of the model, and the texture patches colours are adjusted. This is achieved by adjusting colour between adjacent patches. This results in seamless texture across the model.

G. Data Simulation

The model with texture consists of the path/road and environment (trees and buildings). Lighting, Camera, and Collides are added. Lighting is added to illuminate the model to simulate the light from the sun. The movement of the camera simulates a vehicle moving through the path/road created with the model. The movement gets its inputs from the keyboard. Colliders are Blender3D objects that provide physics attributes to the model, and they are added to prevent the user from moving beyond the required space within the simulator.

IV. RESULTS

The results outlined in this section depict the image rendering framework for the 364 .JPEG images that were captured on each camera at a total dataset worth 2184 JPEG images at a high resolution of 1280X720 pixels at a total size of 39.8MB. The system required a dynamic scene with 6 cameras arranged a 2D arc at a spanning of about 600cm apart from each other. Additionally, each camera frame comprised of 364 JPEG images were captured from the real scene, and only then the process of image matching and texturing is applied using depth maps resulting with the output textured PNG image of 25.2 MB of 8192X9192 pixels resolution.

 ISBN: 978-1-61208-863-1

A. *Rendering Simulation Outcomes*

Figure 8. Denser point of cloud with Multiview stereo.

Following the creation of the mesh output, the texture was then generated by taking models, images, and the camera position (this was achieved through the use of the GPS coordinates). This was accomplished in the meshroom function by selecting 8192 texture slides and by unwrapping this method as indicated in Figure 8.

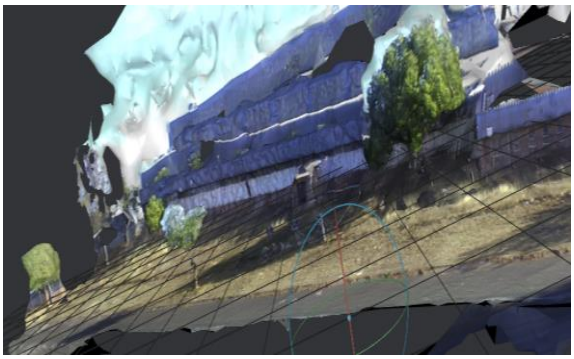

Figure 9. Generated texture.

Figure 9 depicts the depth map restoration and colour images were paired up to create the application of texture to the 3D mesh model and warp to the new viewpoint. Furthermore, the extraction of the depth map model from the 3D mesh, and the shortcomings were observed to be the delay by which the mesh update duration is long and as a result, affects the depth map extraction.

The final output that is represented in Figure 10 depicts the rendered view of the panoramic street views. The panoramic street view can be viewed in multiple viewing angles as indicated in Figure 10.

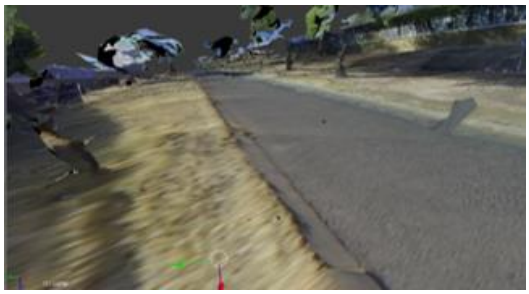

Figure 10. Rendered image horizontal view.

Figure 10 outlines the achieved and projected rendered 3D image from a horizontal street view in an omnidirectional manner. These results are outlined to provide the Freedom of Movement (FoM) and the views which were not captured by the camera but through rendering the uncaptured scene can be viewed.

V. CONCLUSION

The feature detection and matching technique was observed as the best technique in detecting and matching the images from multiple image datasets. As a result, the use of the image-based rendering technique utilising hexagon camera configuration was proposed as an ideal method in this paper.

As compared against the literature, this paper has additionally contributed to the end-to-end process from the development of an image capturing model to rendering a scene with and being able to move forth and back and view the scene that was not originally captured.

Furthermore, the paper has demonstrated the feasibility and efficiency for the integration of the IBR model from a hexagon camera configuration model, and the simulator as indicated:

- The incorporation of the system into the simulation system in real-time for increasing the reality of the simulation system in different geographical locations;
- To simulate a rendering technique for improvement of visual, spatial, and quality of the panoramic images for location identification.

ACKNOWLEDGMENT

Acknowledgment for financial assistance and academic assistance from the Central University of Technology, Free-State (CUT, FS) and Mr. T.G Kukuni for his academic expertise and unending support.

REFERENCES

[1] L. Yin, Q. Cheng, Z. Wandy and Z. Shao, "Big data for pedestrian volume: Exploring the Sasol," Exploring the use of Google street view images for pedestrian counts, no. 63, pp. 337-345, 2015.

[2] N. Runge, P. Samsonov, D. Degraen and J. Schoning, "No more autobahn: Scenic route generation using Googles Street View," In Proceedings of the I, 7-10 March 2016.

[3] R. Sato, S. Ono, H. Kawasaki and K. Ikeuchi, "Photo-Realistic Driving simulator using Eigen Texture and Real-Time Restoration Techniques by GPU," vol. 6, no. 2, p. 87, 2 December 2008.

[4] N. N. Vo and J. Hays, "Localizing and Orienting Street View Using Overhead Imagery," p. 2, 2016.

[5] J. Sivic, B. Kaneva, A. Torralba, S. Avidan and W. T. Freeman, "Creating and Exploring a Large Photorealistic Virtual Space," Proc. IEEE Workshop on Internet Vision, 2008.

 ISBN: 978-1-61208-863-1

[6] J. Kopf, B. Chen, R. Szeliski and M. Cohen, "Street slide: Browsing Street Level Imagery," ACM Trans. Graphics, vol. 29, no. 4, 2010.

[7] S. J. Gortler, R. Grzeszczuk, R. Szeliski and M. F. Cohen, "The Lumigraph. In Computer Graphics Proceedings, Annual Conference Series," in ACM SIGGRAPH, Proc. SIG-GRAPH 96, New Orleans, 1996.

[8] A. Agarwala, M. Agrawala, M. Cohen, D. Salesin and R. Szeliski, "Photographing long scenes with multi-viewpoint panoramas," ACM Transactions on Graphics 25, pp. 853-861, 3 August 2006.

[9] K. Moule and M. McCool, "Efficient bounded adaptive tesselation of displacement maps," In proc. of GI, pp. 171-180, 2002.

[10] H. Y. Shum and S. B. Kang, "A review of image-based rendering techniques," p. 1.

[11] P. E. Debevec, C. J. Taylor and J. Malik, "Modeling and Rendering Architecture from photos: A Hybrid geometry- and image-based approach," In ACM SIGGRAPH, pp. 11-20, 1996.

[12] H. Yuan and R. Veltkamp, "A 3D photo-realistic environment simulator for mobile robots," IEEE Robotics and Automation, vol. 6, no. 2, p. 143, 2021.

[13] Z. Wang, Q. Wang, K. Genora, P. Srinivasan, H. Zhou, J. Barron, R. Brualla, N. Snavely and T. Funkhouser, "IBRNet: Learning multi-view Image-based Rendering," p. 1, February 2021.

 ISBN: 978-1-61208-863-1

Structuring Air Logistics Networks in the Urban Space

Felix MORA-CAMINO
Durban University of Technology, DUT
South Africa, Universidade Federal Fluminense, UFF
Brazil and NMS Lab, Neometsys, France
email: moracamino@hotmail.fr

Bruno LAMISCARRE
NMS Lab, NeoMetSys
Toulouse, France
email: bruno.lamiscarre@neometsys.fr

Georges MYKONIATIS
Ecole Nationale de l'Aviation Civile
Université Fédérale de Toulouse / ENAC
Toulouse, France
email: georges.mykoniatis@enac.fr

***Abstract*— The paper considers the rather unexplored problem of designing a network that can be associated with an urban airspace so that Unmanned Air Vehicle (UAV) based logistics can be performed efficiently. This problem is important to guarantee mobility and accessibility for all operators. First, a structure for the lower layers of the urban airspace is proposed, then an optimal network design problem is formulated, and a heuristic solution approach is developed. The paper is related to the subjects of the Smart Cities and the Smart Mobility of the SMART2021 Conference.**

Keywords: ***UAV; Urban Air Mobility (UAM); Logistics; Graph theory; Optimization and Heuristics.***

I. INTRODUCTION

UAV networks have been considered in the recent literature and are mainly related to either mobile communication networks, based on fleets of UAVs or with route generation for delivery services with UAVs. Important perspectives for the development of urban logistics based on the operation of UAVs are consolidating according to recent publications [1], [2], [3], [4] and [5]. They will be able to take profit of the until now unused urban airspace and so to alleviate ground traffic by diminishing the needs for ground-based logistic transportation which is one of the main contributors to ground urban traffic congestion and pollution.

Previously, many studies have been devoted to the design of efficient UAVs based urban logistics systems, see for example [6], [7] and [8], where in general, traffic volumes and capacities are not taken as issues. However, other studies [9] expect, in few decades, high traffic densities of drones operating in the common urban airspace, making imperative and urgent its effective design and organization.

In this study, the development of a design method for the definition of a network of air links to operate traffic flows of UAVs devoted to urban logistics is considered. While designing this network, the main considered design objectives are: to ensure mobility, accessibility and safety, to master traffic safety, network capacity and environmental impacts. The considered problem presents specific characteristics with respect to traditional urban ground transportation network design problems or with respect to air transportation network design problems, so new solution approaches should be developed. Then, the network structure can be optimized so that equipment and operational costs for end-users are minimized in an efficient way.

This paper is organized as follows: First, an overview of recent UAV systems technology of interest in urban logistics operations is displayed, then assumptions about operational objectives for UAV based logistics in the urban airspace are proposed, leading to a structuring proposal for the whole urban airspace. Then the optimization problem of the operated network inside the urban airspace is formulated and a solution approach is developed and illustrated.

II. OVERVIEW OF UAVS SYSTEMS TECHNOLOGY

The fast technological development (electrical engines, navigation systems and communication devices) and increased availability of commercial UAVs have boosted the use of UAVs to perform many tasks which were until recently, either impossible, or difficult or too costly [10]. Today, commercial UAVs which can be acquired at low cost, when comparing with manned rotorcraft, are used in many different fields, such as surveillance of ground traffic, inspection of buildings and works, agriculture monitoring and resource preservation, search and rescue, meteorology, mapping and photography. Recent UAV technology is offering a large range of fully autonomous rotorcraft, admitting payloads from 1.5kg to 350kg, and mission endurance from half an hour to up to a full working day [11]. Autonomous navigation is available through data fusion which combines information from different sensors for use on board the aircraft. Now on-board computer vision provides on-line localization and mapping, allowing autonomous navigation even

 ISBN: 978-1-61208-863-1

when Global Positioning System (GPS) signals are hidden or jammed [12].

On-board task scheduling (defining the sequence and timing of assigned tasks), path planning (defining the optimal segments of flight satisfying some constraints such as obstacles and no-flight zones), flight parameters trajectory generation (built from the selected path), autonomous control (actions to control UAV angular attitude, including stabilization and robustness with respect to wind perturbations) and autonomous guidance (actions to control center of gravity motion) are already available. Communication with the ground allows trajectory monitoring while communication with other UAVs allows coordination and collision avoidance [13].

The Civil Aviation Authorities around the world are editing regulations to integrate UAVs traffic into the civil airspace (see [14], [15], [16] and [17]). Each authority develops its own regulations but general rules (EASA or FAA) are already established with respect to maximum flight level (flights below 400 feet above ground level), daytime operation or visual flight rules, minimum distance to airports (5 miles). According to the type of activity, specific restrictions will be in use (authorized paths and locations, time of day, operational conditions and in general safety parameters).

There have been some reports concerning UAV crashes on populated areas resulting in property damages as well as in human or animal injuries. Moreover, a significant number of proximities of UAVs with commercial airplanes have happened, even if until today no collision has been reported (see [18] and [19]). Also, there are some concerns by population about the possible loss of privacy which can result from surveillance applications of UAVs. Hence, there is a pressure on governments from media and civil associations to better regulate the use of UAVs in public airspace. Today, different urban logistics applications are under study: general purchase delivery, general mail, pharmaceutical and medical equipment delivery, urban equipment inspection, ground traffic control; it is worth to mention that today, many private and public companies have considered using UAVs as delivery and collection vehicles in the urban airspace. This solution may appear cheaper, faster and more reliable alternative solution than ground-based delivery:

- It is exempt of ground traffic accidents and congestion hazards;

- It does not contribute to the ground traffic congestion as it is the case, significantly, with the ground delivery/collection vehicles.

Pioneer in this sector is the Amazon company that started using rotorcraft UAVs to deliver small packages (up to five pounds) from its logistics centers (up to ten miles to the delivery point). Other applications consider the use of UAVs taxiing to deliver packages directly between particulars. The current regulations do not permit such use, but the increased public acceptance of this new technology and the strong interest and pressure of economic sectors should lead to new regulations enabling urban use of UAVs as it is already the case for traffic surveillance applications. More recently, the Unmanned Aircraft System (UAS) Traffic Management (UTM), a concept developed by the National Aeronautics and Space Administration (NASA) and the Federal Aviation Administration (FAA), and the U-space, a concept developed by the European Union Aviation Safety Agency (EASA), Eurocontrol and the Single European Sky ATM Research (SESAR) Consortium (ATM standing for Air Traffic Management), aims to enable the operation of drones both in the airspace already controlled by Air Traffic Control (ATC) and in uncontrolled airspace today (airspace G), see [20], [21] and [22]. This sector of the airspace that goes outside airport areas and other restricted areas, from the ground level up to 1200 feet in height, generally includes the urban airspace that is the target of this research.

After the COVID19 crisis, a rapid resumption and sustained growth in air transport are expected, and the component relating to urban air transport, which is practically nonexistent today, is foreseen to grow enormously. Eurocontrol's air traffic expectations (total hours flown and total kilometers traveled) for the situation in 2050 in the urban space of Europe, is of about 250 million flights and 15 billion kilometers traveled [23].

III. ADOPTED ASSUMPTIONS AND OBJECTIVES

In this section, we will detail our assumptions, the logistics demand characteristics and the main objectives and constraints of our study.

A. UAVs assumed characteristics for logistics operations

The main predictable operational characteristics of UAVs to be used in urban areas should be:

- Medium to low flying speed (less than 50 m/s) according to propulsion and flying technology (in general rotorcraft);
- Adoption of a common speed V_L inside the movement slice;
- High maneuverability allowing to perform tight turns and vertical flight level changes;
- Full navigation coverage of urban area through onboard integration of vision, ground references and GPS segments;
- Autonomy in guidance along planned trajectories with centimeter accuracy;
- Autonomous collision avoidance capability;
- Small/medium payload capability;
- On board loading/offloading interfaces;
- Soft landing capability in case of failure or damage.

B. Demand characteristics

It corresponds to a mix of point-to-point deliveries and hub and spoke system of deliveries. The point-to-point deliveries correspond mainly to the deliveries between two entities and their volume is expected to be much smaller than the one relative to the hub and spoke system of deliveries which correspond to collective urban services, either public or private. It is supposed that the goods delivered by air from a hub are either produced there or brought by ground bulk transportation to the hubs. It is also considered that with the currently existing

 ISBN: 978-1-61208-863-1

technology, the ground bulk transportation to large distribution centers will remain attractive from the economic and environmental points of view. The demand has a stochastic nature and is distributed spatially and temporally. For planning purposes, it will be considered origin-destination matrices representative of the demand over a given period of time, typically one hour.

C. Main objectives and constraints

When designing the urban air logistic traffic network (L-network), the main constraints to be taken into consideration are the following:

- The designed L-network should provide reachability for any origin-destination pair associated with a demand for logistic UAVs services. In the case of compact urban areas this will imply connectivity of the graph underlying the traffic network.

- The designed L-network is a capacitated network where each link capacity is supposed to be able to cope with its planned traffic.

The two main objectives are:

- The designed L-network should minimize investment, this can be assessed by its total weighted length, where the weight is related to the installed capacity.

- The designed L-network should also propose for each demand a minimum "length" connection as a path of the underlying graph. Length here is a generalized length which can consider either distance, delay or a mix of them. The links constituting this network should be published, dimensioned, delimited and secured with respect to aircraft failures and landing sites and equipped with docking facilities, navigation guides and electrical charge stations. To minimize the costs related to the equipment of the network a set of corridors, fed by secondary links, will be defined.

These two objectives are antagonists, since the second objective should lead to a multiplication of the links of the network and then to an increased investment. Other objectives are relative to safety and environmental impacts which should be minimized. Safety will be the result of the required functional characteristics of the UAVs and of protections installed along with the network (for example when a link crosses a street).

IV. Structuring the Urban Airspace

The decision problem considered here is relative to the design of the traffic management system for UAVs devoted to logistics in urban areas. A basic assumption of this study is that urban logistic air traffic is organized along with the communication links of the urban area (avenues and streets) while the urban passenger traffic is organized between the top of buildings (public and private) and open areas such as parks, cemeteries, outdoor parking areas.

Some reasons in pro of this organization are the following:

- The demand of the end users for urban logistics services is distributed along with the streets network of the cities.

- The introduction of UAVs for logistics should reduce the pollution level in the streets due to ground delivery/collecting vehicles and it can be expected that they will be able to accommodate this new source of disturbance.

- The physical interface of many buildings is through their front, right in the street, and it is doubtful that any historical city may accept to modify notably its architecture.

- The main objectives of passenger air transportation services are to offer a faster and safer means of transportation between origins and destinations inside and outside towns, so it will take place in the open airspace with few obstacles (only the highest buildings).

- The urban passenger air traffic flows will be completely segregated from other means of transportation and from logistics traffic flows, avoiding collision risks with other aircraft.

- The integration of urban passenger air traffic inside the UTM or the U-space will appear to be natural and will be performed more easily.

When the logistic air traffic occupies the lower levels of traffic, two slices can be considered: one for movement along the streets and one for local loading/unloading maneuvers. Here it is supposed that urban passenger traffic occupies the upper levels of the urban airspace with exceptions in open areas which are forbidden for the logistic air traffic. Figure 1 gives a view of the possible organization of a section of the vertical space of a two ways street where air logistics and air passenger traffic are completely segregated. It is supposed that this design remains constant all along a street section. There the two ways are distinguished by the + and – signs. Areas NL+/- represent the two spaces assigned to normal movement at speed V_L, they can contain one or more lanes. Areas UL+/- represent the two spaces assigned to upper crossing maneuvers while LL+/- represent the two spaces assigned to lower crossing maneuvers. These spaces are only present at the proximity of a crossing where conflicts are planned to be avoided by level change maneuvers (Figure 2 displays such a situation). These areas also allow to adapt the flight levels when two successive street sections have different dimensions in their vertical sections. Narrow lateral spaces along the previous areas allow changes of levels without interacting with the level traffic. The areas LUML+/- are dedicated to UAVs maneuvers towards and from logistics terminals or UAVs refueling/maintenance stations. Some areas, in general at the tops of the buildings, are dedicated to Passenger UAVs take-off and landing (PTOL).

In Figure 1, $HLOP_{min}$ and $HLOP_{max}$ are the minimum and maximum AGL levels (AGL: Above Ground Level) for logistics UAVs manoeuvers for docking/undocking, $HLMV_{min}$ and $HLMV_{max}$ are the minimum and maximum AGL levels for logistics UAVs flight progression, $HPMV_{min}$ and $HPMV_{max}$ are the minimum and maximum AGL levels for Passengers UAVs flight progression.

Let H_{max} be the maximum height of the buildings adjacent to a given street section and let h = min {H_{max}, 150ft}, possible values for the different levels can be such as:

$HPMV_{max}$= 400ft, if h=150ft then: $HLMV_{max}$= $HPMV_{min}$= 150ft, if 90ft< $h \leq 150ft$ then: $HLMV_{max}$= $HPMV_{min}$= h , if

 ISBN: 978-1-61208-863-1

$h \leq 90ft$ then: $HLMV_{max}$= $HPMV_{min}$= 90ft, $HLOP_{max}$= $HLMV_{min}$ = 30ft, $HLOP_{min}$ = 10ft.

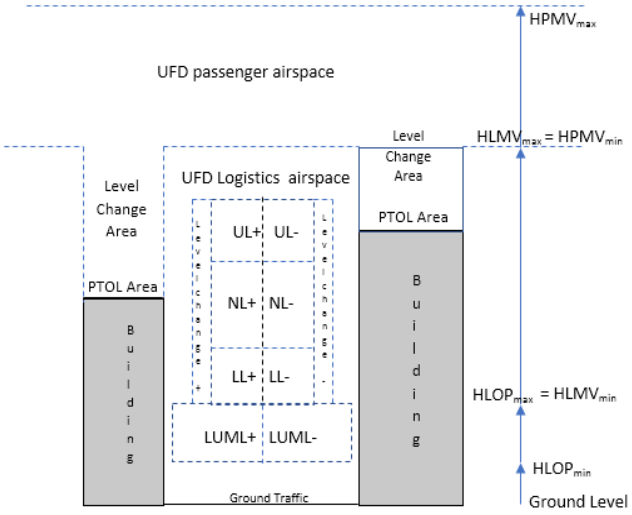

Figure 1: Proposed organization of the street airspace.

In the case of ground traffic, crossings and connections between different street segments create hard crossing conflicts and the adopted solution for nearly a century has been to install traffic lights systems which are costly to install, maintain and operate and which generate traffic queues and waiting times, increasing the direct cost of travel. To avoid this situation in highways with large volumes of traffic operated at high speed, costly civil constructions must be built to avoid cross conflicts. In the case of UAVs traffic, a simple solution is to pre-assign a different flight level to some movements to allow them to cross without any conflict. For example, as shown in Figure 2, any cross conflicts can be avoided by performing no level change for the blue movements, a climb to an upper level for the red movements and a descent to a lower level for the green movements. Note that four convergence conflicts remain, but they can be solved easily by implementing some priority or metering rule.

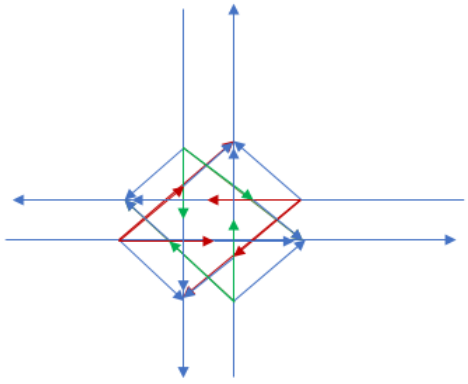

Figure 2: A 3D zero crossing conflict solution at a two ways streets intersection (blue: fly level, red: fly over, green: fly below).

A. *Modelling and structuring urban airspace*

The map of the streets with their intersections with other as well as the position of every building and its connections with the street system are basic data for this study. From the street network is generated a non-oriented graph (it is supposed that every UAV link is two ways) where the set of nodes X_0 corresponds to the street intersections and the set of edges U_0 is associated with the set of sections of streets between two intersections.

From this graph are removed the nodes and edges associated with areas where logistic air traffic is not allowed for any reason such as those related with safety or environment issues, giving way to the graph $[X_1, U_1]$ which is representative of the air street network. The borders of these forbidden areas could be protected by geofencing if necessary.

Considering each building in the urban area, most of them will be connected to the air links of the air logistic network. Each possible connection of the buildings to the air logistic network will represent a user's point connected at both ends of each adjacent edge as shown in Figure 3.a and Figure 3.b. There, the polyhedrons represent the buildings (origin and destination of logistics trips) and the double arrows represent the connection points for logistics.

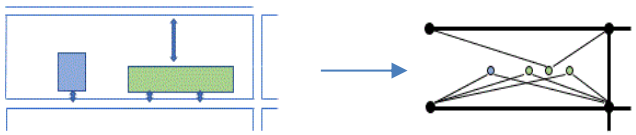

Figure 3a: Graphical representation of connection of end-users with several street sections.

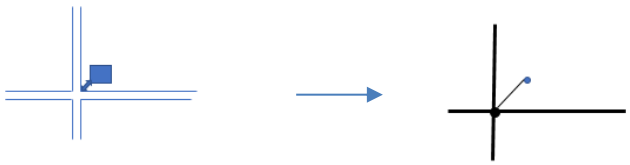

Figure 3b: Graphical representation of connection of end-users with a crossing.

When a distribution or collecting center is located outside the limits of the urban area under consideration, this center and its connections with the urban street systems must be considered too. Then, adding the connection points and the connecting edges as new nodes and edges we get the graph $[X_2, U_2]$. Let also, $X_{OD} = X_2 - X_1$ be the set of origin and destination nodes associated with providers and end-users of the air logistic system.

To each edge (i, j) of $[X_1,U_1]$ can be attached an instant capacity cap_{ij} which is equal to the maximum number of UAVs which can be present in each direction of the street link at a given time. Then the total capacity of link (i, j), CT_{ij}, during a period of time T is given by:

 ISBN: 978-1-61208-863-1

$$CT_{ij} = cap_{ij} \cdot V_L \cdot T / L_{ij} \quad (1)$$

where L_{ij} is the length of the link (i, j). The cost C_{ij} associated with an edge (i, j) of $[X_1, U_1]$ is taken proportional to its length L_{ij}, while the cost of connection of end-users to $[X_1, U_1]$ is proportional to their position in the street section (see Figure 3a).

B. Modelling demand

The considered demand for logistic transportation is represented by a set of origin-destination matrices giving the volumes of trips for different periods of the day between nodes of X_{OD}. Origins and destination of trips can be logistic centers, public offices, shops and restaurants, client positions (for return trips or transfer trips within a distribution tour or a dial-a-ride delivery service). Round trips are broken down into several trips. These origin-destination matrices, written M_T, when covering a short period of time T are asymmetric, but for longer time periods, they tend to symmetrize. Then, they can be written as the sum of symmetric and asymmetric matrices $M_T = MS_T + MA_T$.

V. UAVs Network Optimization

To further reduce the number of air links which have to be equipped, it appears necessary to foresee how the air logistic network will be used, then the air links who are not origin or destination of demand as well as not used by any path between an origin and a destination, can be removed. Also, the flows of air links with very low traffic can be reassigned to other paths so that these air links can be deleted, however, global connectivity of the air logistic network must remain.

A. Formulation of the Optimal Design Problem

First here is considered the optimization problem for users from a central point of view:

- Let P_{ij} be the set of elementary paths linking the origin i and the destination j in the air logistic network of graph $[X_2, U_2]$.
- Let U_{ij}^k be the set of edges composing the kth path between i and j.
- Let CP_{ij}^k be the cost of the kth path between i and j in X_{OD}:

$$CP_{ij}^k = \sum_{(h,l) \in U_{ij}^k} C_{hl} \quad (2)$$

- Let $[a_{ij}^{khl}]$ be the incidence matrix between the k^{th} path between pair (i, j) and air link (h,l): $a_{ij}^{khl} = 1$ if (h,l) belongs to the kth path between i and j, otherwise, a_{ij}^{khl}=0.

Here, no saturation effect is considered and the total cost to be minimized is given by:

$$\sum_{i \in X_{OD}} \sum_{j \in X_{OD}, j \neq i} \sum_{k \in P_{ij}} CP_{ij}^k \cdot x_{ij}^k \quad (3)$$

under the constraints of capacity of the edges of U_1:

$$\sum_{i \in X_{OD}} \sum_{j \in X_{OD}, j \neq i} a_{ij}^{khl} \cdot MT_{ij} \cdot x_{ij}^k \leq CT_{h,l} \quad (h,l) \in U_1, h \neq l \quad (4)$$

and

$$\sum_{k \in P_{ij}} x_{ij}^k = 1 \quad i, j \in X_{OD}, i \neq j \quad (5)$$

with

$$x_{ij}^k \in \{0, 1\} \quad k \in P_{ij}, \quad i, j \in X_{OD}, i \neq j \quad (6)$$

Here constraints (4) are capacity constraints for all the edges of the air logistic network, constraint (5) assumes that all the demands between the pairs i, j of X_{OD} use only one path and constraints (6) recall the binary nature of the considered decision variables.

Then if a solution is obtained, those links composing a used path (path k^* between i and j when $x_{ij}^{k*} = 1$) will be retained for proper equipment in the air logistic network.

However serious difficulties appear:

- The above optimization problem may not have a feasible solution when considering the capacity constraints and the demand levels. A necessary condition to ensure the satisfaction of the capacity constraints (4) is the following:

$$\exists k \in P_{ij} : \max MT_{ij} \leq \min CT_{kl}, \ (k,l) \in P_{ij}^k, \ i, j \in X_{OD} \quad (7)$$

- Problem (3)-(4)-(5)-(6) will be, even for a rather medium size town, a very large Boolean linear program with hundreds of thousands of variables whose numerical application will be extremely expensive in terms of computing time, and this is bad news when different scenarios of demand may have to be tested. So, another approach must be found to efficiently design the air logistic network.

B. Heuristic Solution Approach

Here a greedy heuristic is considered (see [24]) where the larger logistics demands are treated first and assigned to their minimum cost paths taking into account their capacity. So, the steps are the following:

- a) Compute the minimum cost paths between the pairs (i, j) of X_{OD}, the Floyd algorithm can be used here even if its complexity is in $O(n^3)$ where n is the cardinal of X_1, the computational burden can be also diminished by considering some peculiarities of the structure of the considered graph (for instance the presence of sub-trees).
- b) Rank by decreasing logistics demand levels the pairs (i, j) of X_{OD}.
- c) Assign according to this ranking demand MT_{ij} to the minimum cost path between i and j. If there is a capacity overflow at some edges of the minimum path, reallocate on this path a portion of demand equal to the minimum capacity of the edges of this path, then reassign the rest of demand between i and j on the air logistics network without the already saturated edges, repeat the process until all pairs i, j have been treated.
- d) Compute for each edge in the air logistics network its resulting flow F_{kl}, $(k, l) \in U_1$ by adding up the flows in the paths which contain that edge. In this case it can be easily shown that this procedure has a polynomial complexity which is compatible with the computation of real size problems.
- e) A threshold F_{min} can be considered so that the edges such as $F_{kl} < F_{min}$ are deleted from the air logistic network unless they insure connectivity. An algorithm which detects if an edge is a bridge in a graph can be used to point out

which edges, satisfying the above condition, will not be deleted. Then deletion must be done edge by edge while checking current connectivity.

If no edge is removed, the process ends, otherwise, update U_1 and restart the steps from *a* to *e* but only for the pairs (*i*, *j*) which made use of the deleted edges.
Then, once this structure is established, when a new demand for a logistics flight is requested with the urban air traffic management system, a time window and minimum cost path computed within this air logistics network whose loading state should have been updated, will be assigned to the UAV.

C. Illustration of the Heuristic on a Small Scale Case

Here a small size street network represented by a graph of 22 nodes (circles in blue) and 34 edges (blue segments), is considered as given in Figure 4. Table 1 provides the length of the different street sections in meters and the air trips demand matrix *MT*, between 8 origin-destination nodes (the green squares), is given in Table 2.

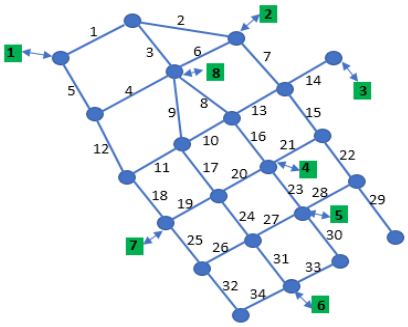

Figure 4: The considered street network.

TABLE I. LENGTHS OF THE STREET NETWORK EDGES.

edges	1	2	3	4	5	6	7	8	9	10	11	12	13	14	15	16	17
length	100	130	100	100	100	100	120	110	110	70	70	100	100	120	90	90	90
edges	18	19	20	21	22	23	24	25	26	27	28	29	30	31	32	33	34
length	90	70	100	100	100	100	100	100	70	100	100	120	90	90	90	100	70

TABLE II. DEMAND MATRIX.

O-D	1	2	3	4	5	6	7	8
1	-	10	5	5	0	5	10	0
2	10	-	0	5	0	0	0	5
3	5	0	-	10	5	0	2	5
4	5	5	10	-	10	5	5	5
5	0	0	5	10	-	5	3	2
6	5	0	0	5	5	-	2	2
7	10	0	2	5	3	2	-	2
8	0	5	5	5	2	2	2	-

After assignment of air trips to their shorter connection path, it appears (see Table 3) that edges 4, 7, 15, 21, 22, 28, 29, 30, 32, 33 and 34 are not used, so they are retrieved from the air logistics network. The reduced graph is displayed in Figure 5.

TABLE III. DISTRIBUTION OF FLOWS IN THE AIR LOGISTICS NETWORK

edges	1	2	3	4	5	6	7	8	9	10	11	12	13	14	15	16	17
flow	25	10	15	0	10	10	0	27	9	2	2	10	27	27	0	32	9
edges	18	19	20	21	22	23	24	25	26	27	28	29	30	31	32	33	34
flow	12	9	10	0	0	17	14	3	3	8	0	0	0	19	0	0	0

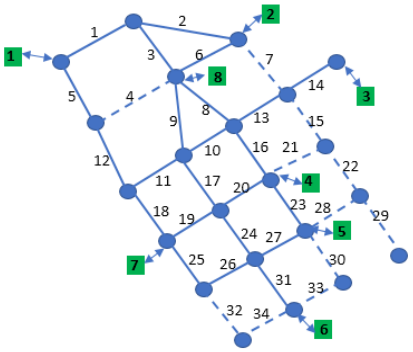

Figure 5: First reduction of the air logistics network.

Then, a minimum flow level F_{min} is chosen, leading to the suppression of low traffic edges. For instance, when F_{min} is taken equal to 9, this leads to the suppression of edges 10, 11, 25, 26 and 27 and the reassignment of their flows along new paths, giving the new flow distribution displayed in Table 4 and Figure 6.

TABLE IV. FINAL DISTRIBUTION OF FLOWS IN THE AIR LOGISTICS NETWORK.

edges	1	2	3	4	5	6	7	8	9	10	11	12	13	14	15	16	17
flow	25	10	15	0	10	10	0	27	9	0	0	10	27	27	0	34	9
edges	18	19	20	21	22	23	24	25	26	27	28	29	30	31	32	33	34
flow	12	17	23	0	0	28	19	-	0	0	0	0	0	19	0	0	0

So, with this heuristic process the number of street sections in the air logistics network is reduced by 44% while less than 5% of total traffic is submitted to an increase of the travel time inferior to 30%.

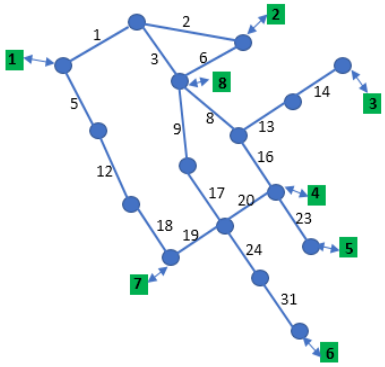

Figure 6: Final air logistics network generated by Heuristic.

VI. CONCLUSION AND FUTURE WORK

This study has considered the design of a network of urban airways allowing mobility and ensuring accessibility to operate traffic flows of UAVs devoted to general logistics over an urban

area. The proposed method makes use of classical concepts and algorithms of graph theory and since the exact optimization problem is in practice intractable for real size problems; a heuristic solution approach that is more computer friendly is developed.

The proposed approach remains preliminary since detailed regulations with respect to the use of UAVs in urban areas are still to be issued. It appears already that a systematic approach such as the one described in this communication leads to a feasible modeling and optimization, it should be completed by custom made rules to make the design more effective and more efficient; also a validation by simulation at the scale of a whole city would be useful to complete this feasibility study.

ACKNOWLEDGMENT

This study was partially funded by the National Council for Scientific and Technological Development (CNPq)-Brazil, Process306663/2020-1.

REFERENCES

[1] Bhawesh S., Rohit Gupta R. and Bani-Hani D., « Analysis of barriers to implement drone logistics », International Journal of Logistics Research and Applications, DOI: 10.1080/13675567.2020.1782862, Published online: 23 Jun 2020.

[2] Eun J., Song B. D., Lee S. and Lim D. E., "Mathematical Investigation on the Sustainability of UAV Logistics," Published: 25 October 2019, Sustainability — Open Access Journal , ISSN 2071-1050.

[3] Goodchild, J. A. and Toy, A., "Delivery by drone: an evaluation of unmanned aerial vehicle technology in reducing CO2 emissions in the delivery service industry," Transp. Res. Part D: Transp. Environ., 61 (2018), pp. 58-67.

[4] Park, J., Kim, S., and Suh, K., "A Comparative Analysis of the Environmental Benefits of Drone-Based Delivery Services in Urban and Rural Areas," Sustainability 2018, 10, 888.

[5] Koiwanit, J., "Analysis of environmental impacts of drone delivery on an online shopping system," Advances in Climate Change Research, 9(3), 201-207, 2018.

[6] Roca-Riu M. and Menedez M., « Logistic deliveries with Drones. State of the art of practice and research », STRC-19th Swiss Transport Research Conference, Ascona, May 15 – 17, 2019.

[7] Iranmanesh S., Raad R., Raheel M. S., Tubbal F., and Jan T., « Novel DTN Mobility-Driven Routing in Autonomous Drone Logistics Networks », DOI 10.1109/ACCESS.2019.2959275, published December 2019.

[8] Zubin I., Van Arem B., Wiegmans B. and Van Duin R., « Using Drones in the Last-Mile Logistics Processes of Medical Product Delivery : A Feasible Case in Rotterdam », https://www.researchgate.net/ publication /338838869 , January 2020.

[9] Doole M., Ellerbroek J., Hoekstra J., « Drone Delivery: Urban airspace traffic density estimation », https://www.researchgate.net/publication/ 329444426, December 2018.

[10] DHL, "Unmanned aerial vehicle in logistics, a DHL perspective on implications and use cases for the logistics industry", http://www.dhl.com/en/ about_us/logistics_insights/dhl_trend_research/lshc2020.html, 2014.

[11] Atkins E., "Autonomy as an enabler of economically-viable, beyond-line-of-sight, low-altitude UAS applications with acceptable risk. In AUVSI unmanned Systems, 2014.

[12] Máthé K. and Busoniu L., "Vision and Control for UAVs: A Survey of General Methods and of Inexpensive Platforms for Infrastructure Inspection Sensors," vol. 15, pp.14887-14916, 2015.

[13] Gageik N., Benz P., and Montenegr S., "Obstacle Detection and Collision Avoidance for a UAV With Complementary Low-Cost Sensors," IEEE ACESS.2015.2432455.

[14] Bart E., "Unmanned Aircraft Operations in Domestic Airspace: U.S. Policy Perspectives and the Regulatory Landscape," Congressional Research Service 7-5700, https://www.fas.org/sgp/crs /misc/R44352.pdf, 2016.

[15] EASA, "Proposal to create common rules for operating drones in Europe," http://easa.Europa.eu/drones, 2015.

[16] Barrado C., Boyero M., Brucculer L.i, Ferrara G., Hately A., Hullah P., Martin-Marrero D., Pastor E., Rushton A. P., and Volkert A., "U-Space Concept of Operations: A Key Enabler for Opening Airspace to Emerging Low-Altitude Operations,"Aerospace2020,7, 24;doi:10.3390/aerospace7030024.

[17] Civil Aviation Department of Hong Kong, "Guidelines on Operations of Unmanned Aircraft Systems (UAS)", http://www.cad.gov.hk/english model_aircraft.html, 2017.

[18] Belcastro, C.M., Newman, R.L., Evans, J.K., Klyde, D.H., Barr,L.C., and Ancel, E., "Hazards Identification and Analysis for Unmanned Aircraft System Operations," In Air Transportation Integration & Operations (ATIO)– Aerospace Traffic Management (ATM) Conference, 2017.

[19] Barr, L.C., Newman,R.L., Ancel,E., Belcastro, C. M., Foster, J.V., Evans, J.K., and Klyde, D.H., "Preliminary Risk Assessment for Small Unmanned Aircraft Systems," In Air Transportation Integration &Operations(ATIO)– Aerospace Traffic Management(ATM) Conference, 2017.

[20] ICAO, https://www.icao.int/safety/UA/Documents/UTM-Framework%20Edition%202.pdf

[21] FAA, June 4 2020, https://utm.arc.nasa.gov/index.shtml

[22] NASA, "Unmanned Aircraft Systems Traffic Management, Concepts of Operation, V2.0," March 2020, https://utm.arc.nasa.gov/docs/ 2020-03-FAA-NextGen-UTM_ConOps_v2.pdf

[23] Eurocontrol, https://www.eurocontrol.int/unmanned-aircraft-systems

[24] Mora-Camino F., Modélisation, Optimisation, Complexité et Algorithmes, in French, Centre National des Arts et Metiers, 2010, Toulouse.

 ISBN: 978-1-61208-863-1

A Data-Driven Approach for Region-wise Environmental Health and COVID-19 Risk Assessment Scores

Sanjana Pai Nagarmat, Saiyed Kashif Shaukat
Research & Development Centre
Hitachi India Pvt. Ltd.
Bangalore, India
email: {sanjana,saiyed.shaukat} @hitachi.co.in

***Abstract*—High population density in India has led to rapid influx of citizens into urban cities. With urbanization, cities are facing massive issues in terms of improving citizen health and living conditions, medical infrastructure facilities and overall environmental conditions. The recent COVID-19 pandemic further threw light on the need to solve these pre-existing challenges. Academic scholars, researchers and industries across the country have developed several platforms and smart city applications to help city planners. However, the data sources largely remain segregated. Due to this, applications have restricted ability to provide interpretable results and quantified scores at a granular level. Our paper introduces a novel data-driven approach that helps city planners easily comprehend the current situation and further prioritize action plans to solve urban challenges of environmental health and medical infrastructure facilities in city wards. Data from several sources are combined to provide scores at a granular ward level that is indicative of ward environmental health and ward level risk in situations like the pandemic. Health score provides recommendations to improve the environmental health while the risk score helps in identifying critical zones and predicting the number of active patients in the region. Several Machine Learning based scoring models to predict risk scores for wards are considered. Risk scores are analyzed on a spatio-temporal basis and results are validated with the actual data from Pune smart city. The model introduced in this paper based on Gradient Tree Boosting Algorithm successfully predicts the ward risk scores with 94.55% accuracy.**

***Keywords*—COVID-19; air quality index; tree cover; health score; risk score.**

I. INTRODUCTION

The urban population in India is one of the fastest growing in the world. With more than half of world's population living in cities, there is tremendous attraction and focus towards planning and development of cities. There is increased connectivity as people and cities are getting smarter. However, this rapid urbanization is causing several problems including environmental degradation, excessive air pollution, deforestation, insufficient water availability, waste-disposal problems, poor healthcare facilities and so on. These issues are further strengthened by the significantly increasing population density, unprecedented events and requirements of the urban cities. There is an ardent need for solutions that quantify and provide insights about these issues at a granular level. These solutions can further aid city planners prioritize and resolve the issues faster.

With increased population in India, Health care systems in particular faced tremendous challenges during the *COVID-19* pandemic [1]. Providing medical care to the citizens became challenging due to grappling shortage of medical facilities and infrastructure [2]. The need to primarily prioritize health care facilities in cities became crucial. However, no method provided granular information in the cities to help anticipate the required medical facilities. Also, there were no solutions or applications which helped city planners predict the risk associated with anticipated number of patients in the cities.

The Government of India has already started several initiatives to promote urbanization and growth in a sustainable manner. Smart city project is one such initiative that is focussing on the development of 100 smart cities across the country. Pune, a sprawling city in the western Indian state of Maharashtra has received funding from the Government of India to develop under this initiative. To tackle the problems of urbanization via adoption of next generation technologies and solutions, the *Pune Smart City Development Corporation Limited (PSCDCL)* was formed on 23rd March 2016 in Pune. Together with the *India Urban Data Exchange (IUDX)* [3], an open source data exchange platform aimed at enabling cities to harness full potential of the enormous data being generated in the smart cities, Pune launched the *Pune Urban Data Exchange (PUDX)* [4] pilot and exposed about 850 databases via the IUDX APIs. Apart from PUDX, the *Pune Municipal Corporation (PMC)* [5] has also created the Pune datastore with around 450+ datasets related to varied sources including but not limited to information and technology, environment, transport, healthcare facilities etc. The intention behind this is to mainly promote problem-solving, co-creation among stakeholders to create sustainable outcomes in Pune.

In-spite of several data platforms and data sources being available, the data is segregated and siloed. Data aggregation becomes necessary to gain deeper and meaningful insights from it.

 ISBN: 978-1-61208-863-1

This paper presents a novel data-driven approach that combines several relevant data sources, creates data rich models to improve the environmental conditions of the city, its medical infrastructure and to provide better quality of life to its citizens. The work is based on the data from PMC region in Pune. PMC is the civic body that governs the inner limits of Pune spread over an area of 331.26 sq.km. Based on the 2011 census, the data from 144 wards of the PMC region is considered in this study [6]. However, the same approach can be applied to other smart cities as well. Contributions of this work are as follows:

- **Combining and utilizing rich feature set to provide ward-wise environmental health scores and recommendations**: Rapid urbanization has led to drastic deterioration of Pune's natural heritage. Low-density suburbs rich in greenery have morphed into neighbourhoods congested with high-rises [7]. This has negatively affected environment, climate, overall health and biodiversity in Pune. To help authorities get a wholistic view of the environmental health at a granular ward level in PMC-Pune [8], we provide a data-driven scoring and recommendation model. Environmental attributes like air quality, tree cover and population of wards in the PMC region are used to formulate a score that indicates ward level environmental health. Relevant data features from Pune sources are selected and sub scores are calculated to compute the final health score. Further, based on the health score a recommendation is provided to increase the green tree cover of the region. We also developed an interactive user dashboard to visualize the results.
- **Investigating the environmental attributes, their trends and variations during the COVID-19 pandemic**: Impact of the COVID-19 pandemic over the various environmental attributes including Air Quality Index (AQI), sound, ozone, $N0_2$ and particulate matters (PM_{10}, $PM_{2.5}$) are studied. Variations of these attributes are quantified over time and relevant screens are implemented to help user easily understand and interpret the results.
- **Aggregated data rich models that provides dynamic ward level risk scores**: PMC faced grappling shortage of staff and medical facilities during the COVID-19 pandemic due to lack of planning [2]. A novel data-driven scoring mechanism to indicate ward level risk is implemented. Rich data sources that provides ward level information related to air quality levels, tree cover, population density, hospital and medical infrastructure facilities and pandemic related information are combined, relevant features are selected and latest data available is utilized to formulate the score dynamically. The numerical score provided by the system represents the medical health status of the ward which is indicative of the number of predicted active COVID-19 cases in the ward. The risk scores not only indicate the ward status but can also be used to compare wards and gain deeper insights.

Overall the work in this paper provides granular ward level details and localized information dynamically considering the change in the attributes. The scores proposed in this work can help provide adequate information to concerned authorities to plan and implement control measures. It will also guide them to prioritize and identify potential high-risk wards. Further, map-based representation of wards to effectively provide spatio-temporal information about ward health, environmental attribute variations and risk levels is provided to relay information in an easily understandable manner to the users.

The remaining part of the paper is organized as follows. Section 2 discusses the related work. Section 3 describes the technical information pertaining to the data sources, score computations, recommendations, detailed analysis with suitable graphs and plots. Section 4 presents the results and discussions while Section 5 describes conclusion of our approach.

II. Related Work

Related works that analyse the environmental attributes like the air quality index and the tree cover independently in Pune exist. These works separately analyse the attributes and present approaches to optimize the environmental conditions. Kane et al. [9] studied the scope and opportunity in Pune to understand the green cover for maintaining a balanced floral diversity. While National Research Development Corporation [10] studied the air quality in Pune to develop an air information response plan. These previous approaches study the environmental attributes independently and do not provide any kind of scoring mechanisms to quantify the findings. In our work, we provide a wholistic view of the environmental health at a *granular ward level* in Pune. We formulate a relative health score for the ward by combining several attributes – *air quality index, tree* and *human population*. Morani et al. [11] provide a planting index for a location by analysing the associated tree cover. It makes use of Geographic Information System (GIS) based visual approximation techniques to estimate the green tree cover. Our work utilizes the air quality, population and the surveyed tree data from PMC-Pune to provide an index that indicates the ward health. The publicly available geo-sensor based surveyed tree information is used in the calculation of green tree cover rather than the approximation techniques used in [11]. We then aggregate the tree information at a ward level, combine several tree attributes to score the trees and utilize this sub score in computing the environmental health score. Based on the ward health, our method goes one step ahead by providing recommendations on how the score can be used to further improve the green tree cover in the area.

Sharma et al. [12] studied the effect of restricted emissions during COVID-19 on air quality in India. In our work, we investigate the trends of air pollutant concentrations at a granular ward level in PMC-Pune during the COVID-19 pandemic. Such granular details at ward level will help ward authorities take specific actions on areas under their jurisdiction.

Yaro et al. [13] studied and evaluated the impact of some selected demographic and environmental variables to identify potential risk areas and hotspots for COVID-19 transmission. The primary focus of this work was to identify statistically

 ISBN: 978-1-61208-863-1

significant hotspots for further transmission of COVID-19 specifically in Nigeria. In our work, we make use of the ward level medical infrastructure details, ward demographics, environmental variables like air quality, tree data and the existing hotspots information to collectively provide a single numerical indicator of risk at a ward level. Our work is based on data from PMC-Pune region.

III. Methodology

This section provides details on the data sources, formulation of scores along with dashboard visualizations.

A. Environmental Health Score Formulation

1) Data Sources: To provide a relative measure of understanding the environmental ward health, health scores are computed by combining air quality, tree details and population data.

- *Air Quality data* [14]: The PUDX platform provides data related to the air quality sensors installed in several parts of Pune city. 50+ sensors installed across the city actively measure the concentrations of pollutants. The sensors provide AQI readings every 15 minutes. A pipeline is created and a job to collect this data on a regular basis is scheduled. The collected sensor data is then mapped to the appropriate wards.
- *Pune Tree Census data* [15]: PMC has mapped over 40 lakh geo enabled trees using GIS technologies and made data available to the public. It includes data of tree attributes like height, girth, width, botanical names, ownership details, location information and so on.
- *PMC Population breakup of administrative wards* [16] : Census is conducted once in every ten years in India. It provides information at the root level. The Pune city census office is responsible to carry out the census activities effectively and efficiently in the PMC area. The administrative ward level detailed census data in Pune is made available to the public by the PMC.

2) Score Formulation: Health score is formulated using air quality, population and tree data. The trees in the PMC-Pune region are studied. Based on their importance and contributions towards the environment, individual tree scores are calculated. From the literature survey, we found out that evergreen trees planted in rows can capture up to 85% of the particulate air pollution blowing through their branches. In addition, a single tree produces nearly three-quarters of the oxygen required for a person and a canopy of trees in an urban environment can slash smog levels up to 6% [17]. We also studied the local tree species, their ideal height and girth requirements to come up with weights that will help in scoring the individual trees. Based on our investigation, four important tree attributes i.e. height of the tree (in meters), its physical condition (poor, average, healthy), phenology (seasonal, evergreen) and its canopy diameter (in meters) are selected and used to score each tree (Tree_Value).

$$\begin{aligned} Tree\_Value = w1(Height) + w2(Canopy) \\ + w3(Phenology) + w4(Condition) \end{aligned} \quad (1)$$

Here weights w1, w2, w3 and w4 are calculated with respect to Table I. We have assumed that taller and healthier evergreen trees with wider canopies provide more contribution towards a green buffer zone. Also, evergreen trees are more economical requiring less maintenance when compared to seasonal trees.

The trees are mapped to appropriate wards based on geo coordinates. According to an Indian Institute of Science (IISc) report [18] from 2014, the ideal tree-human ratio should be seven trees for every person. With this reference, if a ward has **n** trees we calculate the Tree_Score as a ratio of sum of all the individual tree scores in the ward to the ideal tree score (Ideal_Tree_Score).

$$Tree\_Score = \frac{\sum_{i=1}^{n} Tree\_Value(i)}{Ideal\_Tree\_Score} \quad (2)$$

$$\begin{aligned} Ideal\_Tree\_Score = Max\_Tree\_Score \\ * Ward\_Population * 7 \end{aligned} \quad (3)$$

Max_Tree_Score is the maximum score that can be assigned to a tree based on Table I. The upper bound for the Tree_Score of a ward is set to 1. In several smart cities, health check for the trees are done by authorities on a regular basis. They periodically make a note of tree health and changes in their conditions if any. Such periodically updated information can be used in calculating more appropriate tree scores.

The AQI score is calculated by utilizing the dynamic AQI values provided by PUDX every 15 minutes. For wards with sensors installed, we take an exponential moving average [19] (decay constant is calculated based on the number of AQI observations in a span of one month) of AQI values for individual sensors, calculate the mean of this value for all the sensors available in that ward and then normalize the mean value with respect to the maximum AQI value (considered as 500).

$$AQI\_Score = \frac{(Max\_AQI\_Value - AQI\_Value)}{Max\_AQI\_Value} \quad (4)$$

For wards where air sensors are not available, we have used approximations to get the AQI value at a ward level. We identify five nearest sensors (based on PMC sensor locations, five sensors are available on an average in the vicinity of a ward) to these wards, take an average of their AQI value and assign it as the AQI value of the ward. Geo-coordinates and spherical boundary calculations are used here to identify the nearest sensors [20].

To account for the increase in population over the years, in our work we have studied the average population growth in Pune and made interpolations to the actual population census data collected in 2011. For calculating the population score, we first calculate the population density of the wards. Then, the value is normalized with respect to the ward that has maximum population density in the PMC region (Max_Density).

 ISBN: 978-1-61208-863-1

TABLE I
WEIGHTS FOR TREE ATTRIBUTES

w1		w2		w3		w4	
Height	***Score***	***Canopy***	***Score***	***Condition***	***Score***	***Phenology***	***Score***
0-3m	0.2	0-1m	0.2	Poor	0.25	Seasonal	0.3
3-5m	0.4	1-3m	0.4	Average	0.5	Evergreen	0.7
5-8m	0.6	3-5m	0.6	Healthy	0.75		
8m+	0.8	5m+	0.8				

$$Population\_Score = \frac{(Max\_Density - Ward\_Density)}{Max\_Density} \quad (5)$$

Once the scores (Tree_Score, AQI_Score and Population_Score) are calculated for all the wards, they are combined with a weight factor [11] and normalized on a scale of 0 to 100 as shown in (6).

$$Health\_Score = (Tree\_Score * 30) + (AQI\_Score * 40) + (Population\_Score * 30) \quad (6)$$

3) Plots and Visualization: Figure 1 shows the health scores for wards in PMC region. Health scores are numeric values in the scale of 0-100. Wards are categorized into zones (Extremely poor (0-20), Poor (20-40), Moderate (40-60), Satisfactory (60-80) and Good (80 and above)) based on the values of the health score.

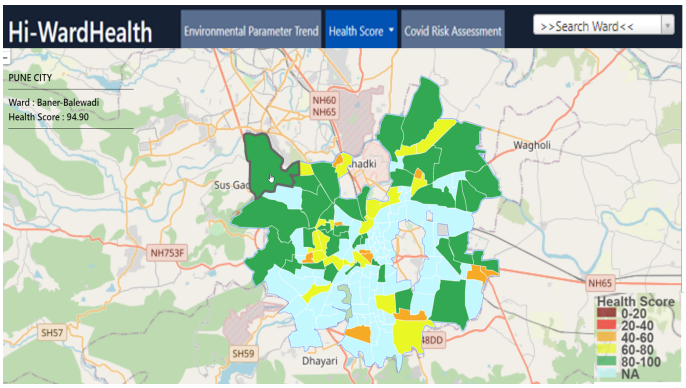

Figure 1. PMC-Pune Ward Health Scores.

4) Green Buffer Zone recommendation and example: For any selected location within the PMC region, recommendations to further improve the green cover of that place is provided. For a selected location and a boundary area around it, the attributes (air quality, tree count, population density) are analysed to compute an environmental health score based on (6). Our technique also goes one step beyond this by providing recommendations for the construction of green buffer zones. The green buffer zone recommender system at the backend compares the health score of a place with a pre-defined threshold value (80 by default). If the health score is less than the threshold and Tree_Score is less than 1, recommendation to further improve the green tree cover of the place is provided to the user. To improve the health score of a place to at least the predefined threshold, the recommender system provides insights on the number of trees that must be planted (until Tree_Score upper bound of 1 is not reached) as shown in Figure 2.

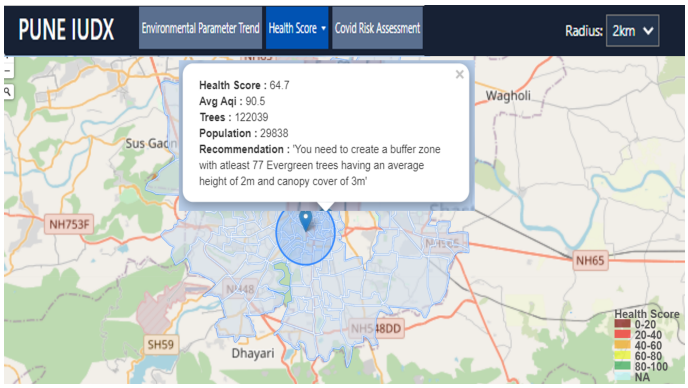

Figure 2. Green Buffer Zone Recommendation.

5) Health Score usability: We have calculated the health scores for PMC-Pune wards where data is available. Higher value of health score indicates better ward health. Table II shows health scores, tree count, population and AQI levels for some wards.

TABLE II
HEALTH SCORES OF PMC-PUNE WARDS

Ward Name	Health Score	AQI	#Trees	Population
Baner-Balewadi	94.8	54.1	207671	150190
Ved Bhavan	92.2	80.4	115324	171906
Lohagaon Vimantal	91.9	111.2	293974	163064
Mundhvagaon	91.0	94.4	160422	90815
V Mahavidhyalaya	90.5	98.0	81776	68110
S Mahavidhyalaya	90.0	106.3	19766	73811
Fergussion College	89.0	114.9	50105	76911
Magarpatta Hadapsar	89.0	83.8	25203	193003
Sadhana Vidhyalaya	88.5	93.5	22666	135103
Kothrud Gaon	86.8	103.2	72851	90671
RajBhavan	85.6	123.6	5084	88484
Shanivarwada	82.3	133.8	54499	61042
PhuleNagar Yerwada	81.7	160.2	125254	78268
Koregaon Park	81.1	111.7	5458	71299
AundhGaon	68.2	93.2	7663	83859
D.P Dattawadi	65.8	83.5	42050	83026
S.G Rugnalya	63.7	103.3	3071	86535
Tingre Station	62.2	83.2	4336	111015

 ISBN: 978-1-61208-863-1

Of the 63 wards, we noticed that 12 wards had moderate health scores, 15 had satisfactory scores and 36 wards had good scores. With the health score, it becomes easy to identify wards with poor environmental health. Health score can help:

- Real estate owners decide selling and buying price of properties across wards depending on its environmental conditions.
- Government to impose certain restrictions on vehicular movements in highly polluted wards.
- Authorities to grant or deny permissions for further construction activities in wards based on their health conditions.

B. Study of variations of environmental attributes during COVID-19

With the onset of COVID-19 cases in India, the Government of India imposed a complete nationwide lockdown [21] starting from March 25th, 2020 which restricted people from stepping out of their homes. All transport services - road, air and rail were suspended during the lockdown phase. We studied the various environmental parameters like AQI, Sound (in db), Ozone, Particulate Matters ($PM_{2.5}$, PM_{10}) and NO_2 across thirty-one PMC-Pune wards over a period of four months (January 2020 to April 2020) and quantified their variations. Average parameter variations observed across PMC-Pune wards include:

- 41.0% decrease in AQI level
- 3.0% decrease in Sound level
- 70.3% decrease in PM_{10} level
- 83.7% decrease in $PM_{2.5}$ level
- 82.5% decrease in NO_2 level
- 77.5% increase in Ozone level

This significant decrease in various attributes can be contributed to suspension of activities and restrictions imposed on citizens during the lockdown. Residential areas showed significant reduction in attributes like AQI, sound and pollutant concentrations with the imposition of lockdown. However, since few essential services continued their operations during this phase, we could see variations in reduction of attributes across wards. Based on the data avaiable from PUDX, sample AQI variations of one of the residential wards: Phulenagar both day-wise and month-wise is shown in Figure 3 and Figure 4 respectively.

This study helps concerned authorities plan and prioritize control measures to improve the quality of air in PMC-Pune. Figure 5 shows a dashboard that helps users visualize the variations and trends of these attributes. They can compare wards and visualize the trends of the environmental attributes over time using this dashboard. Figure 6 shows a dashboard that helps users visualize the ward-level attribute variations and trends in further detail. They can also analyse the ward level variations on a daily, weekly or monthly basis.

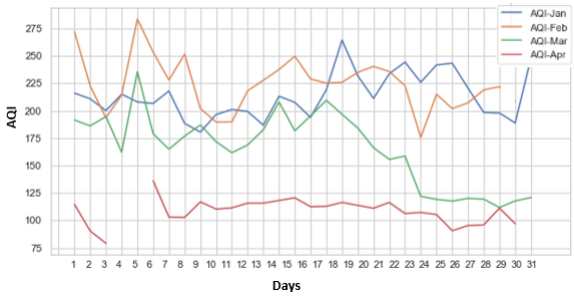

Figure 3. Day-wise AQI variation in Phulenagar.

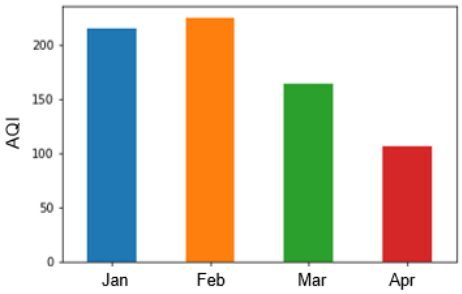

Figure 4. Month-wise AQI variation in Phulenagar.

C. Covid Risk Assessment Score

During situations like the pandemic, providing primary facilities like healthcare to all the citizens becomes the need of the hour. With the steady increase in the COVID-19 cases, PMC faced grappling shortage of healthcare staff and hospitalization facilities over time [2]. With the influx of patients from rural areas into the cities, the hospital management faced tremendous pressure in providing medical help. Thus, we propose a solution that will help concerned authorities get ward level insights for planning further development of medical facilities in wards and to be better prepared in situations like this. Our solution assesses the overall health and medical infrastructure facilities available at a ward, formulates a risk score and provides ward specific insights. A prediction model learns from rich sources of data and predicts a risk score that is correlated to the anticipated number of active patients in the ward. Finally, based on the risk scores the wards are categorized into risk zones. This categorization helps concerned authorities take prioritized decisions with respect to ward administration.

1) Data Sources:

- *COVID hospitals and bed details* [22]: A detailed list of hospitals and the number of beds allocated to treat COVID-19 patients that is updated on a day-to-day basis is collected using web scrapping techniques.
- *Additional hospitals* [23]: Provides a list of additional healthcare facilities and the number of beds available in PMC-Pune region.
- *Demographics* [24]: Publicly available information like - number of literates, number of children below age 6,

 ISBN: 978-1-61208-863-1

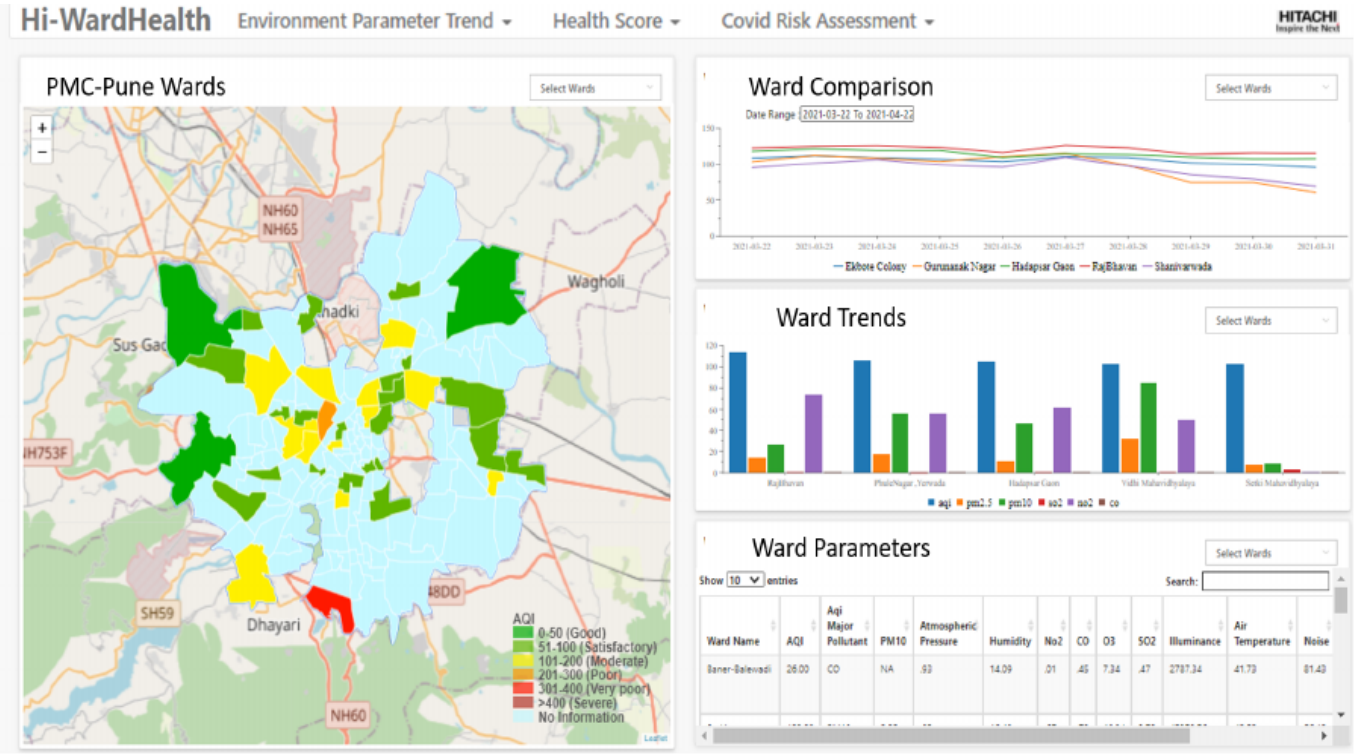

Figure 5. PMC-Pune city Environmental Attributes trend and variations.

working population and average family size in a ward is collected from the data source.

- *Hotspots* [25]: Information about the critical zones in the PMC-Pune region with COVID-19 cases is provided. Data is extracted using relevant APIs.
- *Environmental health scores*: The ward wise health scores formulated based on AQI, tree and population count mentioned in Section 3.1.3 is used.

2) Modelling System and Score Formulation: To predict the ward risk score, firstly, a pipeline is created, and a job is scheduled for periodic data collection. This is followed by data pre-processing, data aggregation and model building. In the first step, data is collected from all the above-mentioned data sources on a day-to-day basis. Next, in the pre-processing step, the geo-coordinates and addresses available in the collected data is mapped to appropriate ward IDs using geocoding and mapping techniques. Further, in the data aggregation step, based on ward IDs the data is aggregated at a ward level.

We studied an extensive set of environmental and demographic factors that are important attributes in contributing to ward risk at times like the pandemic. Based on the literature survey, thirteen relevant features as shown in Table III are selected to train our model. However, it must be noted that no single attribute or feature can individually explain the measure of ward risk. Grietens et al. [26] in their work show how factors such as high human mobility rate, age structure, poverty level, high illiteracy and population density as well as dependency ratio have been influencing the transmission dynamics of diseases. As per a study conducted in New York, USA, using Kendall and Spearman rank correlation test, it was found that temperature and air quality had a significant association with the COVID-19 pandemic (Bashir et al. [27]). Air quality, population density along with the green tree cover is formulated as a health score and is used as an important factor in assessing the ward risk (Feature 1) in Table III. Dalziel et al. [28] and Casanova et al. [29] showed that virus transmission can be influenced by several geographical factors such as climatic conditions (temperature and humidity) and population density. Also, as we are aware, the primary means of transmission of the virus is through physical contact as shown in work by Pung et al. [30]. The spread of infection is usually accelerated in crowded conditions.

To account these notable factors and observations, this paper considers demographic factors at ward level that include the number of houses (Feature 2), literate population (Feature 3), population below the age group of 6 (Feature 4), average family size (Feature 5) and working population (Feature 6). Apart from this, the preparedness of any ward in situations like the pandemic, depends upon its ability to provide the required medical facilities. To account this, the information of hospitals (Feature 7) and the bed facilities: beds with oxygen (Feature 8), beds without oxygen (Feature 9), ICU beds with ventilator (Feature 10), ICU beds without ventilator (Feature 11), additional non COVID-19 beds available in medical facilities across PMC-Pune (Feature 12) to treat patients is

 ISBN: 978-1-61208-863-1

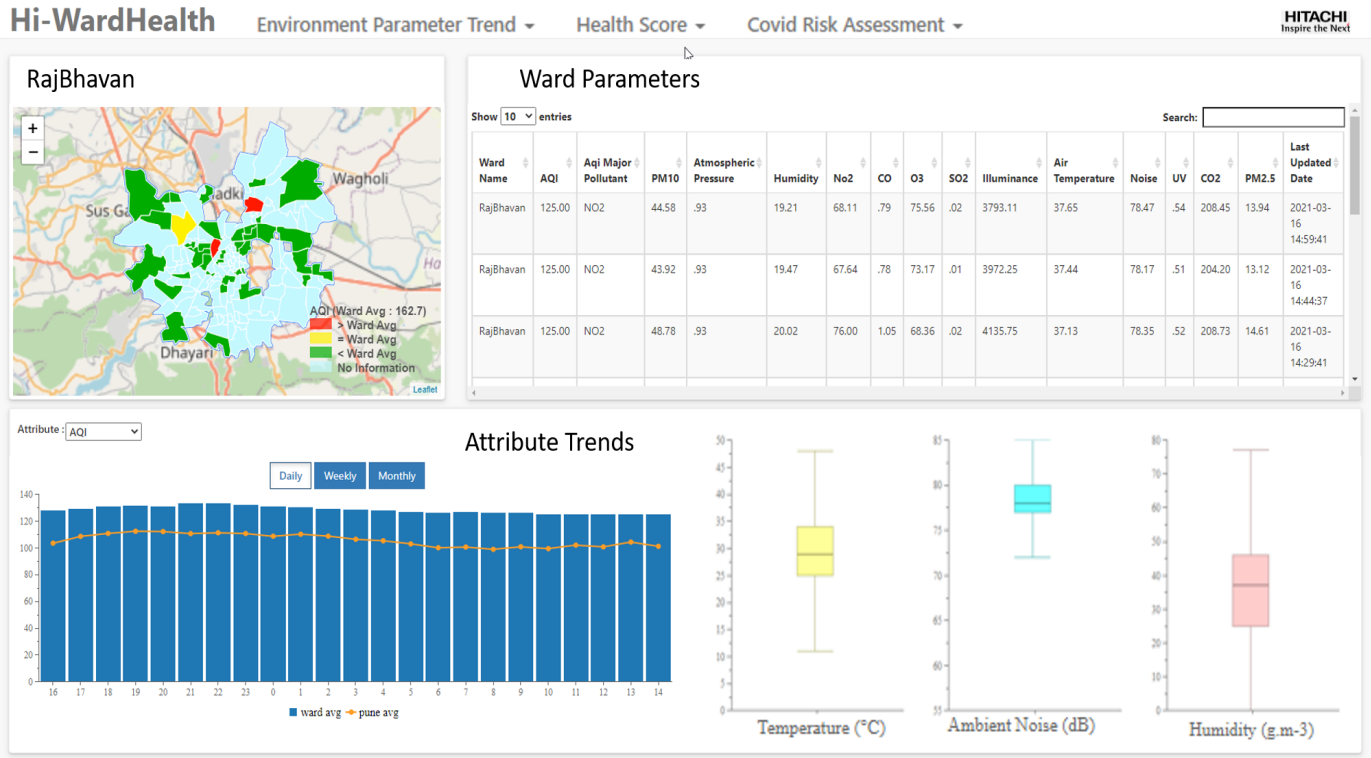

Figure 6. Ward level Environmental Attributes trend and variations.

used. All the features are normalized with respect to the ward population.

TABLE III
FEATURES USED TO CALCULATE THE COVID-19 RISK SCORE

Feature#	Feature Name
1	Health Score
2	Houses
3	Literate Population
4	Population under 6
5	Family Size
6	Working Population
7	Hospitals
8	Oxygen beds
9	Beds without oxygen
10	ICU ventilator beds
11	ICU beds without ventilator
12	Additional beds
13	Hotspots

The data collected for these features over a period of time (November 2020 - December 2020) is used to train the model and the data from January 2021 is used for testing. Models are built to predict ward-wise Risk Assessment Score (RAS) or risk score which is an indicator of anticipated number of active patients for the next day in the ward. Several Machine Learning based prediction algorithms like Linear Regressor, Random Forest, K-Nearest Neighbor and Gradient Tree Boosting are used to predict the risk scores based on the thirteen input features selected. In any ward, more the number of active COVID-19 cases, more is the risk. With this analogy, we calculated the number of active patients per day in a ward, formulated the risk score as a function of category of active patients. Weights are assigned to each of the category of active patients as shown in (7). This is then normalized with the ward population (8) and used as the Initial Risk Assessment Score (Initial_RAS) while training the model.

$$\begin{aligned} Risk\_Sum = 0.1 \ * \ (Patients\ without\ oxygen) \\ + 0.2 \ * \ (Patients\ with\ oxygen) \\ + 0.3 \ * \ (Patients\ without\ ventilator) \\ + 0.4 \ * \ (Patients\ with\ ventilator) \end{aligned} \tag{7}$$

Here, more importance is given to patients currently under ventilator support in the ICUs (weight factor: 0.4) followed by those in ICUs without ventilator (weight factor: 0.3), followed by patients in regular wards with oxygen supply (weight factor: 0.2) and finally the regular patients (weight factor: 0.1).

$$Initial\_RAS = \frac{Risk\_Sum}{Ward\_Population} \tag{8}$$

Based on the thirteen input features (normalized with ward population) and Initial_RAS as the output, the model is trained to predict the Risk Assessment Score (Predicted_RAS) to anticipate the number of active patients on the next day. For evaluation, based on thirteen feature values on current date, the model predicts Predicted_RAS score (which is an indication of active patients anticipated for the next day). This is then compared with Initial_RAS score (8) which is computed based

 ISBN: 978-1-61208-863-1

on the actual patient numbers on the next day. The Root Mean Squared Error of the prediction (Predicted_RAS) with respect to the Initial_RAS score is then compared to select the best performing model. The predicted risk scores are normalized on a range of 0-100, where 0 indicates minimum and 100 indicates maximum relative risk score. Table IV shows Gradient Tree Boosting based predicted risk scores for the wards in Pune. A sample of the risk scores for the wards on January 31st, 2021 is shown. Wards are categorized into five zones based on the value of risk scores - Severe (100-80), High (80-60), Moderate (60-40), Low (40-20), Very Low (20-0). Higher the risk value, greater is the risk.

TABLE IV
WARD LEVEL COVID-19 RISK ASSESSMENT SCORES

Ward Name	Risk Score	Risk Zone
Dhanori	1.9	Very Low
Bopodi	3.3	Very Low
Yerwada Prison Press	6.7	Very Low
Bibvewadi	14.5	Very Low
Renuka Swarup Prashala	16.1	Very Low
Kharadigaon	19.2	Very Low
Yashwantrao Chavan Natyagraha	23.2	Low
Bharti Vidhyapeeth	23.5	Low
Dinanath Mangeshkar Rugnalaya	42.7	Moderate
Baner-Balewadi	81.9	Severe

Based on the calculated risk scores as of January 31st, 2021 1 ward showed severe risk, 1 showed moderate, 2 showed low while 18 wards showed very low risk. These relative ward level risk scores can help the authorities take prioritized actions by focussing on wards that require immediate attention. The risk scores of wards also vary over days. Some wards show significant variations while some show minimal variations in the risk levels.

3) Plots and Visualizations: The dashboard shown in Figure 7 help users visualize the ward risk scores and categorize them into zones. Feature values across wards in PMC-Pune along with the hotspot case progression is shown.

The user can also analyse details at a ward level and gain insights on the various features, their values and compare it with the overall PMC-Pune average as shown in Figure 8. With such comparisons, it becomes easier to understand the relative preparedness of the wards.

4) Evaluation: The performance of several Machine Learning models was considered to predict the risk scores. Table V shows prediction errors in risk scores with various Machine Learning algorithms.

The predicted risk score values and their variations for wards across days is studied in detail. The average prediction error rate of models using various machine learning algorithms is compared. Table V shows a sample reference of various models and their performance for 15 days. Gradient Tree Boosting based Regressor shows 5.45% error in prediction when compared to Random Forest Regressor (5.92%), K-Nearest Neighbors (6.01%) and Linear Regressor (22.40%).

TABLE V
PREDICTION ERRORS WITH MACHINE LEARNING MODELS: LINEAR REGRESSION (LR), K-NEAREST NEIGHBORS (KNN), RANDOM FOREST (RF), GRADIENT TREE BOOSTING (GTB)

Dates	LR	KNN	RF	GTB
12-01-2021	23.46	5.49	6.23	5.55
13-01-2021	23.69	3.68	4.38	3.56
14-01-2021	26.11	5.98	6.57	5.87
15-01-2021	23.31	4.72	5.23	4.39
16-01-2021	22.38	4.96	5.53	4.66
17-01-2021	23.70	5.44	6.06	5.35
27-01-2021	32.51	12.75	11.77	10.93
28-01-2021	31.55	11.38	10.34	9.57
29-01-2021	19.67	6.48	4.45	4.18
30-01-2021	19.75	6.79	5.3	4.78
31-01-2021	20.14	7.60	6.11	5.6
01-02-2021	19.52	6.22	4.73	4.19
02-02-2021	16.21	2.82	3.97	4.1
03-02-2021	16.92	3.43	4.57	5.02
04-02-2021	17.11	2.49	3.63	4.07
Average error	**22.40**	**6.01**	**5.92**	**5.45**

Based on the results, Gradient Tree Boosting algorithm is selected to predict the ward level risk scores. The results are further validated with the initial hypothesis which indicated that risk score of the ward is correlated to the number of active cases in the ward. A sample result is shown in Table VI.

TABLE VI
CORRELATION BETWEEN RISK SCORE AND ACTIVE PATIENTS

Ward Name	Predicted_RAS	Active Patients*
Dhanori	1.9	7
Bopodi	3.3	23
Bibvewadi	14.5	43
Yashwantrao Chavan Natyagraha	23.2	76
Dinanath Mangeshkar Rugnalaya	42.7	145
Baner-Balewadi	81.9	599

*per 10000 population.

Ward-wise risk scores can help authorities take planned actions and be better prepared to provide required medical facilities to its citizens in times of need.

IV. RESULTS AND DISCUSSIONS

In our work two scores to indicate the environmental health as well as the risk score for wards in PMC region of Pune are formulated. Out of 144 wards in PMC as per 2011 census, based on data availability, data for 63 wards was collected and scores were derived for them. In case of health scores, AQI information was collected from 33 sensors, tree data from 73 wards and population census data from all the 144 wards. AQI data was interpolated to calculate the health scores of the wards. Out of the 63 wards, 12 showed moderate scores, 15 satisfactory and 36 showed good health scores. Additionally, a few locations in PMC-Pune were also selected to check the environmental health status. Some regions already showed good health scores while some showed satisfactory and poor conditions. For those locations appropriate recommendations

 ISBN: 978-1-61208-863-1

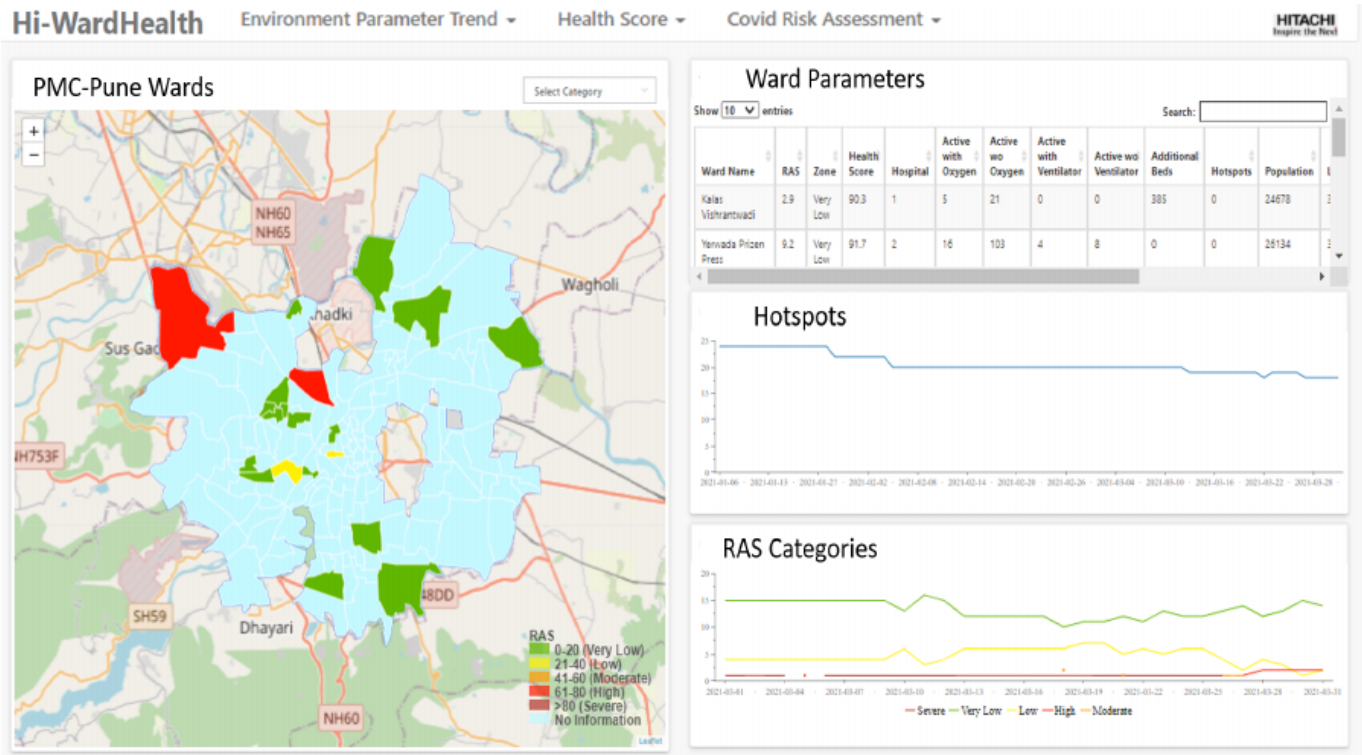

Figure 7. PMC-Pune COVID-19 Risk Assessment Scores.

on the number of trees further needed to improve the health score was provided.

Based on our detailed analysis of environmental parameters during lockdown, a significant decrease in level of pollutant concentrations in Pune was observed. AQI, $PM_{2.5}$, PM_{10}, NO_2 and sound levels showed decrease of 41.0%, 83.7%, 70.3%, 82.5% and 3.0% respectively while Ozone showed an increase of 77.52%. According to a study [31] a high NO_x level reacts with Ozone and mops it up. The Ozone that escapes to cleaner areas has no NO_x to further cannibalize it and as a result, Ozone concentration builds up in these areas. This explains the increase in concentrations of Ozone in the atmosphere.

In case of risk scores, we combined several data sources and collected data for PMC-Pune wards. The combined data available for 22 wards was used to calculate the risk scores. Majority of wards showed low risk scores while a few showed medium risk scores. These relative scores help compare wards and take further decisions to improve the ward level infrastructure and medical facilities.

V. Conclusion and Future Work

This paper provides a data-driven method of modelling environmental health and ward level risk of a city considering the available infrastructure, demographics and the environmental health conditions. Our method utilizes the most recently available data to provide dynamic scores to wards. These numerical scores can be used as an indicator in prioritizing the wards that need more focus than the others. It also gives an understanding of wards at a granular level. A dynamically changing health score index makes an attempt to quickly assess the ward environmental health. It serves as an important indicator that helps city planners improve the environmental conditions of the ward. Our paper also studied the variations of environmental parameters in Pune over a stipulated period of time. Further, a dynamic risk score prediction model is introduced in this paper that combines several relevant sources of data to predict the risk levels of a ward. When the overall condition of a ward improves, its ability to handle situations like the pandemic increases. With better facilities, the living conditions in the ward can improve and the ward can gradually attain self-sufficiency.

The model can be further enhanced by adding valuable features like average hospitalization duration of patients, number of direct contacts and other COVID-19 transmission related information based on data availability. The visualizations presented in this work can be further enhanced by making use of Human Computer Interaction techniques. We also plan to implement a simulator that would help authorities foresee the risk scores in wards with gradual changes in the ward facilities over a period of time. Overall, the scores proposed in this work and its evaluation was done based on the data available in PMC-Pune. However, the same can be extended to other smart cities where similar data is available.

References

[1] COVID-19. https://en.wikipedia.org/wiki/Severe_acute_respiratory_syndrome_coronavirus 2021.05.24.

 ISBN: 978-1-61208-863-1

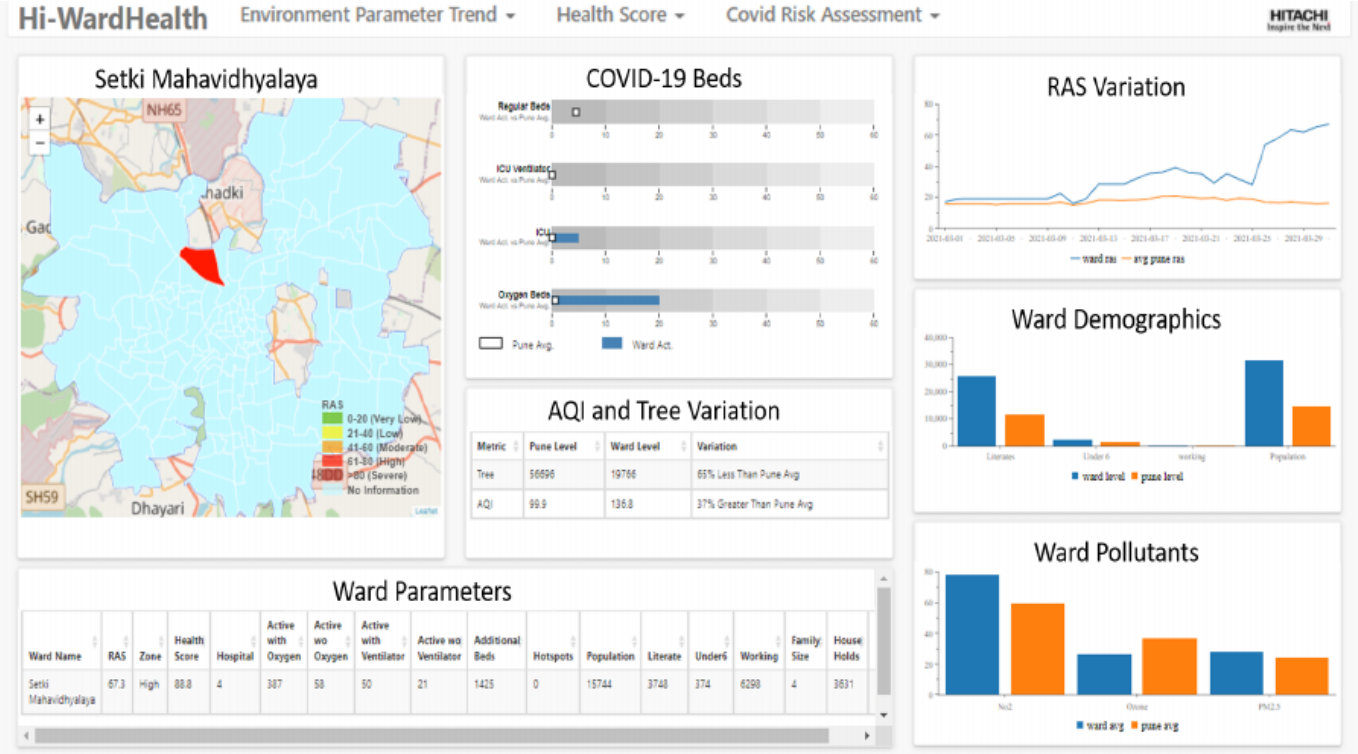

Figure 8. Ward level COVID-19 Risk Assessment Scores.

[2] PMC Healthcare. https://indianexpress.com/article/cities/pune/amid-healthcare-staff-shortage-and-rising-fatigue-overburdened-pvt-hospitals-in-pune-at-breaking-point-6591101/ 2021.05.24.
[3] IUDX. https://iudx.org.in/ 2021.05.24.
[4] Pune IUDX Catalog. https://pune.catalogue.iudx.org.in/ 2021.05.24.
[5] PMC. https://pmc.gov.in/mr 2021.05.24.
[6] Pune wards. https://ourpuneourbudget.in/know-your-city/pre-2012-144-wards/ 2021.05.24.
[7] PMC-Pune ward details. https://www.pmc.gov.in/en/all-ward-office 2021.05.24.
[8] What is Pune losing. https://www.civilsocietyonline.com/cover-story/what-is-pune-losing-and-how-fast/2021.05.24.
[9] A. Kane, V. K. Ganesan, M. Sardesai, and M. Shindikar, "Green Cover Analysis using Tree Census Data to Optimize the Bio-diversity in Pune Municipal Development Area", UDS 2020, vol. pp. 45–56, 2020. doi: http://ceur-ws.org/Vol-2557/.
[10] NRDC. https://www.nrdc.org/sites/default/files/media-uploads/pune_air pollution_ib.pdf 2021.05.24.
[11] A. Morani, D. J. Nowak, S. Hirabayashi, and C. Calfapietra, "How to select the best tree planting locations to enhance air pollution removal in the MillionTreesNYC initiative". Environ Pollut. 2011;159(5): pp. 1040-1047. doi:10.1016/j.envpol.2010.11.022.
[12] S. Sharma et al., "Effect of restricted emissions during COVID-19 on air quality in India. Sci Total Environ. 2020;728:138878. doi:10.1016/j.scitotenv.2020.138878.
[13] C. A. Yaro, P. S. U. Eneche, and D. A. Anyebe, "Risk analysis and hot spots detection of SARS-CoV-2 in Nigeria using demographic and environmental variables: an early assessment of transmission dynamics", International Journal of Environmental Health Research. doi:10.1080/09603123.2020.1834080.
[14] IUDX dataset. https://pune.catalogue.iudx.org.in/search/dataset/items 2021.05.24.
[15] PMC Open Data Store. https://opendata.punecorporation.org/Citizen/CitizenDatasets/Index?categoryId=24&dsId=483&search=tree%20census 2021.05.24.
[16] City census department. https://www.pmc.gov.in/en/census 2021.05.24.
[17] Evergreen tree benefits. https://canopy.org/tree-info/benefits-of-trees/ 2021.05.24.
[18] IISC survey. https://www.asianage.com/metros/mumbai/211217/one-tree-for-every-four-persons-bmc-census.html2021.05.24.
[19] Exponential moving average. https://www.investopedia.com/ask/answers/122314/what-exponential-moving-average-ema-formula-and-how-ema-calculated.asp 2021.05.24.
[20] Finding points within a distance of a latitude/Longitude using bounding coordinates. (n.d.). J. P. Matuschekpage. https://JanMatuschek.de/LatitudeLongitudeBoundingCoordinates 2021.05.24.
[21] Lockdown in India. https://en.wikipedia.org/wiki/COVID-19_lockdown_in_India 2021.05.24.
[22] COVID hospital data. https://www.divcommpunecovid.com/ccsbeddashboard/hsr 2021.05.24.
[23] Additional hospitals. http://opendata.punecorporation.org/Citizen/CitizenDatasets/Index?categoryId=35&dsId=446&search=hospital 2021.05.24.
[24] Demographic data. https://indikosh.com/city/588016/pune 2021.05.24.
[25] Hotspots in India. https://www.covidhotspots.in/ 2021.05.24.
[26] K. P. Grietens et al., "Characterizing types of human mobility to inform differential and targeted malaria elimination strategies in Northeast Cambodia". Sci Rep. 5(1):16837. doi:10.1038/srep16837.
[27] M. F. Bashir et al., "Correlation between climate indicators and COVID-19 pandemic in New York, USA". Sci Total Environ 728:138835. doi:10.1016/j.scitotenv.2020.138835.
[28] B. D. Dalziel et al., "Urbanization and humidity shape the intensity of influenza epidemics in U.S cities". Science 362: pp. 75–79, 2018. doi:10.1126/science.aat6030.
[29] L. M. Casanova, S. Jeon, W. A. Rutala, D. J. Weber, and M. D. Sobsey, "Effects of air temperature and relative humidity on coronavirus survival on surfaces". Appl Environ Microbiol. 76(9): pp. 2712–2717, 2010. doi: 10.1128/AEM.02291-09.
[30] R. Pung et al., "Investigation of three clusters of COVID-19 in Singapore: implications for surveillance and response measures". Lancet. 395(10229): pp. 1039–1046, 2020. doi:10.1016/S0140-6736(20)30528-6.
[31] Air Pollutants COVID-19. https://indianexpress.com/article/explained/covid-19-lockdown-air-pollution-ozone-6479987/ 2021.05.24.

 ISBN: 978-1-61208-863-1

Towards a New Model to Evaluate Smart Mobility in Latin America

Eladio E. Martinez-Toro
Universidad Paraguayo Alemana
San Lorenzo, Paraguay
e-mail: eladio.martinez@upa.edu.py

Augustinus van der Krogt
Universidad Paraguayo Alemana
San Lorenzo, Paraguay
e-mail: stijn.vanderkrogt@srh.de

Carlos G. Samaniego-Orue
Universidad Paraguayo Alemana
San Lorenzo, Paraguay
e-mail: cgsamanieg@gmail.com

***Abstract*—The major metropolitan areas in Latin America are facing a fast-increasing transport crisis in terms of congestion and very long travel times, pollution, accidents, and user safety. Like cities in developed countries, many cities in the region have started smart mobility programs to address these issues. In recent years, many models have been developed to evaluate these programs but most of these models are using indicators that do not consider specific mobility problems in Latin America. This article has identified eight specific regional challenges to mobility and proposes a new model. The model includes a set of specific indicators and metrics that allow researchers to conduct a more realistic and data-driven comparative evaluation of mobility challenges and smart mobility programs Latin American cities.**

Keywords - smart mobility; mobility challenges in Latin America, mobility models.

I. INTRODUCTION

The concept of mobility has been interpreted in a variety of ways. The National Research Council in its report Key Transportation Indicators defines that “mobility refers to the time and costs required for travel” [1]. With the field of mobility, urban mobility is of key importance because the cities are the center of the economic and social activities of human beings [2]. In recent years, there have been important economic, social, and technological changes that led to new models to understand and measure urban mobility. These urban models have been implemented throughout the world considering factors, such as the increase in average distances traveled, changes in the reasons for travel and changes in the location of productive activities [3].

More recently the mobility models have evolved into the smart city model that considers a broader set of indicators. A smart city is characterized by seeking "the promotion of integrated and sustainable development, where cities become more innovative, competitive, attractive and resilient" [4]. The Smart Cities Council Readiness Guide defines a smart city as one that uses Information and Communication Technologies (ICT) to improve its habitability, work capacity and sustainability [5]. Cohen and Obediente [6] propose that smart cities, through the application of technology in their different areas, become more efficient localities in the use of their resources, saving energy, improving the services provided and promoting sustainable development. In its report Smart Cities, Ranking of European medium-sized cities, Giffinger et al. [7], reviewed the common characteristics of several European cities classified as smart and proposed a model defined by six main pillars: smart people, smart economy, smart governance, smart environment, smart living, and smart mobility.

Latin America is the world´s most urbanized developing region, characterized by high levels of economic and social inequality and fast-growing urbanization, resulting in increasing mobility problems [8]. Although some smart mobility and public transport integration projects have begun to be developed in Latin America to address these issues, smart mobility is one of the pending tasks for the region [9].

The evaluation of progress in smart mobility in Latin America is complicated since most of the smart mobility models were developed considering the mobility problems in developed countries. Consequently, there is no model that considers the specific characteristics and challenges of smart mobility in Latin American cities. The objective of this article is to identify a new smart mobility model for Latin America that can serve as the basis for a more effective comparative analysis of urban mobility in the region. To achieve this goal, this article offers a review of the literature of current mobility models and identifies the key indicators and their metrics mobility challenges in Latin America.

In Section II, the general concept of smart mobility is defined and Section III describes a series of Smart Mobility Models and their indicators proposed by different authors. Section IV details the key mobility challenges in Latin American. Section V describes the proposed smart mobility model including indicators and metrics. Conclusions are presented in Section VI.

II. SMART MOBILITY

According to Carballo et al. [10], the concept of smart mobility is defined as the set of actions, techniques and infrastructures that lead to the improvement of mobility and the organization of traffic in cities. The main objective of smart mobility is the use of technology and data for the integration of all actors in displacement, to achieve greater efficiency and sustainability in cities [11]. Smart mobility seeks to address some of these problems through the application of technological tools such as ICT, allowing the establishment of specific objectives. The use of technology in smart mobility allows integrating the data of the road actors to automatically attend to incidents that occur on the routes, prediction and prevention of accidents and some trends in terms of behavior, such as hours and congested routes. In the same way, it is possible to have public transport integration systems, which facilitate connections between

 ISBN: 978-1-61208-863-1

one means of transport and another, while monitoring climatic and environmental conditions [12].

III. SMART MOBILITY MODELS AND INDICATORS

Several researchers have developed smart mobility models that build on a combination of a series of underlying indicators to measure and compare the status of smart mobility in cities at global level. For this research, eleven of the most representative smart mobility models are analyzed as a starting point for the development of a suitable smart mobility model for Latin America. Cohen [13] in his research proposes a mobility index that considers three categories including efficient transport, multi-modal access, and technology infrastructure. Some of the indicators are clean-energy transport, public transport, smart cards, and access to real-time information. The model of Lupiañez, and Fauli [14], evaluates the urban smart mobility projects based on inputs, outputs, and outcomes/impact. The most relevant outcome indicators are the number of personal vehicles per capita, the travel time, transport-related victims per 100,000 inhabitants and the number of public transport services that offer real-time information to citizens.

Battarra et al. [15] compare cities through indicators and smart actions developed in them. The categories evaluated in the model are accessibility, sustainability, and ICT. Each category was eventually divided into actions and these actions were divided in parameters. Aletà et al. [16] propose a model that compare cities through the evaluation of the following factors: sustainable mobility urban plans, integrated payments in multimodal transport systems, deployment of alternative transport modes and the use of ICT in traffic control. The model also proposes measurable direct evaluation metrics. Aini and Amani [17] consider a diversity of indicators classified in the following variables: location efficiency, reliable mobility, health and safety, environmental stewardship, social equity, and robust economy.

The model of Orlowski and Romanowska [18] assesses the infrastructure of cities, their mobility methods and information management infrastructure using the following indicators including indicators on the technical infrastructure, information infrastructure, mobility methods, used vehicles and transport legislation. A complex model for European cities is proposed by Giffinger et al. [7], which evaluates local accessibility, national accessibility, availability of ICT infrastructure and a sustainable, innovative, and safe transport system. Also, the California Department of Transportation defines a series of indicators for smart mobility including location efficiency, reliable mobility, health and safety, environmental stewardship, social equity, and a robust economy [19]. Šurdonja et al. [20] presented a model that consisted of a questionnaire that allows evaluating the main aspects of the ideal model of a smart city.

Factors like those mentioned previously were evaluated in the model proposed by Martinez-Toro et al. [9]. The model proposes five key indicators to evaluate mobility and transport integration including long-term mobility policies, resistance by transport operators to system integration and digital payment, limited use of bank accounts by the population, limited infrastructure in ICT and lack of financial resources to invest in mobility programs. Finally, we can mention the model presented by Berrone and Ricart [21], that evaluates and scores cities in nine main aspects: human capital, social cohesion, economy, governance, environment, mobility and transportation, urban planning, international projection, and technology. In this model the most representative indicators are traffic index, traffic inefficiency index, exponential traffic index, CO_2 emissions, number of particles in the air (PM10 and PM 2.5) and the number of deaths from traffic accidents. The main advantage of the last two models is that it presents most of the Latin American countries, giving in advance an idea of how it would be possible to evaluate them and use the aspects they have developed.

Most of the models that we mentioned above, except for the ones proposed by Martinez-Toro et al. [9], and Berrone and Ricart [21], were developed to evaluate smart mobility in highly developed cities in developed countries and do not consider mobility problems in Latin America as presented in Section II. Therefore, this article seeks to identify a model with the most relevant indicators for the problems identified in Latin America.

IV. MOBILITY CHALLENGES IN LATIN AMERICA

A key challenge to mobility is the advanced levels of urbanization in Latin America, at this moment the most urbanized developing region in the world. A United Nations study expresses that urbanity in Latin America has increased from 40% in 1950 to 80% in 2015 [22]. The high levels of urbanization combined with economic growth has also resulted in a fast level of motorization in the region. This is furthermore combined with a lack of road infrastructure planning in Latin America which leads to an increase in traffic congestion [23].

A further factor of concern is found in the great distances resulting in elevated travel time of citizens within the larger metropolitan areas such as Sao Paulo, Mexico City, Rio de Janeiro, and Lima, which represents great mobility problems in terms of transport time for both higher end and lower income citizens alike. These directly affect the well-being of populations as they must spend more time moving from one place to another to satisfy their social and economic needs [24].

According to a study developed by García [26], public transport allows people with limited resources to leave the precarious residential spaces where they live and the need to move to their places of work or study and to access services that these people need daily. However, the inoperative and incompleteness of the integration of transportation systems result in awfully long travel times and high cost of transport for lower income citizens that need to access work and training opportunities, as well as the services that people need daily to carry out their daily activities, despite some success stories such as the Transmilenio in Bogota, Colombia [26][27]. In many cities in the region people need to take various transport modes (bus, metro, train) that require more than two hours travel time per day. The study published by Martinez-Toro et al. [9] provides a detailed analysis of the

 ISBN: 978-1-61208-863-1

key challenges to the development of integrated and intelligent public transport systems in eight cities in Latin American. The main challenges identified were the resistance by transport operators thus resulting in incomplete physical integration of transport systems and related digital payment options. Also, the limited ICT infrastructure and a lack of financial resources assigned by most Latin American governments to invest in smart mobility programs and policies.

In recent decades, precarious and dangerous transport conditions in Latin America are causing high levels of travel accidents. Today, traffic accidents are one of the leading causes of death in the region, mainly among people between the ages of 5 and 44 [28]. This implies that traffic accidents cause more than 100,000 deaths per year, and approximately more than 5 million people are injured [29].

Traffic congestion and a lack of regulation of the quality, maintenance and age of car vehicles comes with environmental pollution, noise pollution, deterioration in the state of the streets. Traffic congestion and pollution comes with a high level of CO_2 emission from vehicle combustion. As a result, high levels of air pollution in many Latin American cities represents the greatest environmental health risk today, and it is estimated to contribute to 7 million premature deaths each year [30]. According to the 2018 World Air Quality Report published by Greenpeace and IQAir, Lima and Santiago are among the countries with the highest level of air pollution in the world. Peru is ranked 21st in the global ranking, while Chile is ranked 26th [31]. This places Latin America as a major source of pollution, posing a serious problem for the environment and the health of the inhabitants of this continent.

Finally, we find an increasing problem caused by a lack of safety of the users of public transport. According to a study published by Jaitman [32], 50% of women in Lima and Asuncion use public transport as a daily means of travel. At least a third of these women experience unsafe transport conditions and report to have been robbed, insulted, suffered some type of verbal or even sexual assault while traveling with public transport. Another 30% of the women do not report these inconveniences because they do not believe it necessary or due to lack of time.

In summary, to develop a relevant smart mobility model for Latin American cities, a new regional model that considers key indicators from the combination of different factors is needed. In the first place it is essential to consider physical indicators of smart mobility including vehicular congestion, travel times and the presence of an adequate and inclusive ICT infrastructure. Secondly advancement in smart mobility requires sufficient planning capacity of transport authorities and access to financial resources to implement smart mobility programs. Thirdly it is important to consider environmental factors represented by air pollution levels and to consider key indicators on security which can be expressed in the level of traffic accidents and user safety.

V. PROPOSED SMART MOBILITY MODEL FOR LATIN AMERICA

To determine the models that are best suited to evaluate smart mobility challenges and conditions in Latin America, the research team has conducted a detailed analysis of the indicators used by eleven smart mobility models and their relevance for the key challenges of urban mobility in the region. The combined models proposed by Martinez-Toro et al. [9], Lupiañez et al. [14] and Berrone et al. [21] are found to be most relevant to construct a new model to evaluate smart mobility that considers specific challenges and conditions in Latin America. Table 1 presents the proposed model that demonstrates the relation between the key mobility problems in the region, the indicators and metrics that enable future measurement of each indicator.

TABLE I. PROPOSED SMART MOBILITY MODEL FOR LATIN AMERICA

Mobility Problem	Indicator	Metrics	Author
Vehicular congestion	-Traffic index -Exponential traffic index -Traffic inefficiency index	-Average one-way travel time to work in minutes [33] -Estimation of dissatisfaction due to long commute times with exponential levels of dissatisfaction with travel time to work above 25 minutes [33] -Estimation of inefficiencies in travel time caused by transport by private car compared to public transport [33]	Berrone and Ricart, 2020.
	-Number of vehicles	-Number of private vehicles per inhabitant	Lupiañez, and Fauli, 2017.
Time spent traveling	-Travel time	-Additional time needed to 30 minutes of travel distance	Lupiañez, and Fauli, 2017.
ICT infrastructure	-City-wide Internet coverage -Digital transport service platforms with real time information	-Internet penetration rate per inhabitant in the city -Percentage of transport companies with digital transport service platforms that offer real time travel information	Martinez-Toro, et al., 2019.

Transport system and payment integration	-Geographically integrated transport modes -Integrated digital payment systems among transport modes	-Percentage of transport service companies with integrated transport modes -Percentage of transport service companies with integrated digital payment systems among transport modes	Martinez-Toro, et al., 2019.
Financial resources	-Public, private, and multi-lateral investments in mobility programs	-Amount of total investment available for mobility per 100,000 inhabitants per year	Martinez-Toro, et al., 2019.
Environmental pollution	-Emission of CO_2, PM10, and PM2.5	-Emission CO_2 in grams per minute por passenger -Annual average of the number of particles PM10 in the air whose diameter is less than 10 µm. -Annual average of the number of particles PM2.5 in the air whose diameter is less than 10 µm.	Berrone and Ricart, 2020.
Traffic accidents	-Number of deaths in accidents	-Number of deaths in accidents per 100,000 inhabitants per vehicle	Berrone and Ricart, 2020.
User safety	- Public transport services that offer real-time information -Victims related to transportation	-Percentage of public transport companies that offer on-line and real-time travel information -Transport-related victims per 100,000 inhabitants	Lupiañez, and Fauli, 2017.

Source: Own Elaboration

The smart mobility model presented in Table 1 includes the interactions between key regional mobility challenges, their indicators and metrics to measure each indicator. To evaluate the eight mobility challenges, fourteen indicators were selected after the analysis of the most representative existing smart mobility models. The challenge of traffic congestion is measured by the traffic index, the exponential traffic index, the traffic inefficiency index and the number of vehicles. Excessive travel time in cities is evaluated by the additional travel time that is needed to travel in a 30-minute journey.

City-wide internet coverage and the digital transport service platforms with real time information are key indicators to evaluate urban challenges in ICT infrastructure. Problems related to a lack of transport integration can be evaluated by looking at the level of integration of the different transport modes and payment systems. The availability of public, private and multilateral investment in mobility programs represents a good indicator of the challenge of limited access to financial resources. Finally, environmental challenges are compared by the level of CO_2 emission and PM10 and PM2.5 air particles. Transport safety considers the number of fatal traffic accidents and user safety is evaluated to the extent to which travelers can dispose of public transport services that offer real-time information and the number of victims in traffic. The combined set of indicators and metrics provide a new model that considers the specific regional mobility challenges and allows to compare the smart mobility performance between Latin American cities.

VI. Conclusions And Future Work

This study on smart mobility has identified key problems that are relevant to evaluate the progress in smart mobility in urban areas in Latin America. The challenges include the traditional factors related to elevated vehicular congestion and long travel times but also problems related to a lack of integrated transport and payment systems, deficiencies in ICT infrastructure and a lack of financial resources to finance smart mobility programs. Other important factors include air pollution, traffic accidents and user safety.

The research also analyzed eleven models that evaluate smart mobility of which three models were found to be most relevant to evaluate the key smart mobility challenges in Latin America. The models developed by Martinez-Toro et al. [9], Lupiañez et al. [14] and Berrone et al. [21] together provide an accurate set of smart mobility factors and indicators that cover the aforementioned smart mobility challenges in the region.

The new model enables researchers to conduct more realistic and effective data-driven evaluations of mobility challenges and the progress in smart mobility in different Latin American cities. In addition, it allows for the development of a comparative smart-mobility index of Latin American cities. To accomplish this, we propose to set up a panel of experts with representatives of mobility professionals and researchers, government, private industry, and end users. The panel is to validate and assign individual weightings to the model´s indicators and to homogenize the values obtained to have a uniform numerical index that facilitates a more realistic evaluation of smart mobility in Latin America.

References

[1] National Research Council, Key transportation indicators: summary of a workshop, National Academies Press, Washington D.C., 2002.

[2] A. Monzon, "Smart cities concept and challenges: Bases for the assessment of smart city projects," 2015 International Conference on Smart Cities and Green ICT Systems (SMARTGREENS), Lisbon, pp. 1-11, 2015.

[3] C. Miralles-Guasch, City and transport: the imperfect binomial, Ariel, Barcelona. Ciudad y transporte: el binomio imperfecto, Ariel, Barcelona, 2002.

 ISBN: 978-1-61208-863-1

[4] M. Bouskela, M. Casseb, S. Bassi, C. De Luca, and M. Facchina, The Road toward Smart Cities Migrating from Traditional City Management to the Smart City, Inter-American Development Bank, 2016. Available from: https://publications.iadb.org/bitstream/handle/11319/7743/La-ruta-hacia-las-smart-cities-Migrando-de-una-gestion-tradicional-a-la-ciudad-inteligente.pdf. [retrieved: 03, 2021]

[5] Smart Cities Council. The definition of a smart city. [Online]. Available from: https://rg.smartcitiescouncil.com/readiness-guide/article/definition-definition-smart-city. [retrieved: 03, 2021]

[6] B. Cohen, and E. Obediente, Study "Ranking of smart cities in Chile". Estudio "Ranking de ciudades inteligentes en Chile", 2014.

[7] R. Giffinger et al., Smart Cities: Ranking of European Medium-Sized Cities (Centre of Regional Science (SRF), Vienna, 2007.

[8] D. Hidalgo and C. Huizenga, Implementation of sustainable urban transport in Latin America. Research in transportation economics, 40(1), pp. 66-77, 2013.

[9] E. E. Martínez-Toro, A. Van der Krogt, and R. Sanchez-Flores, Mobility and Integration of Public Transport Systems in Latin America. MLMI 2019: Proceedings of the 2019 2nd International Conference on Machine Learning and Machine Intelligence, 2019. https://doi.org/10.1145/3366750.3366760

[10] L. Carballo, A. Villagra, and M. Errecalde, Smart mobility: reduction of gas emissions, Scientific Technical Reports - UNPA, 11(2), pp. 53-69. Movilidad inteligente: reducción de emisión de gases, Informes Científicos Técnicos - UNPA, 11(2), pp. 53-69, 2019. https://doi.org/10.22305/ict-unpa.v11i2.786

[11] E. Ontiveros, D. Vizcaíno, and V. L. Sabater, The cities of the future: smart, digital, and sustainable, Ariel. Las ciudades del futuro: inteligentes, digitales y sostenibles, Ariel, 2016.

[12] I. De la Serna, The new mobility: from the Smart City to Industry 4.0. Towards a new mobility in cities, 62. La nueva movilidad: de la Smart City a la Industria 4.0. Hacia una nueva movilidad en las ciudades, 62, 2020.

[13] B. Cohen, Smart city index master indicators survey. Smart cities council, 2014.

[14] F. Lupiañez, and C. Fauli, Smart Cities: Social evaluation of Smart Cities projects, Center for Telecommunications Studies of Latin America. Ciudades Inteligentes: Evaluación social de proyectos de Smart Cities, Centro de Estudios de telecomunicaciones de América Latina, 2017.

[15] R. Battarra, C. Gargiulo, M. R. Tremiterra, and F. Zucaro, Smart Mobility in Italian Metropolitan Cities: A comparative analysis through indicators and actions. Sustainable cities and society, 41, pp. 556-567, 2018.

[16] N. B. Aletà, C. M. Alonso, and R. M. A. Ruiz, Smart Mobility and Smart Environment in the Spanish Cities. Transportation Research Procedia, 24, 2017.

[17] N. N. Aini, and H. Amani, Indicators to measure smart mobility: An Indonesian perspective, In Proceedings of the 2017 International Conference on Telecommunications and Communication Engineering, pp. 81-85, October 2017.

[18] A. Orlowski, and P. Romanowska, Smart Cities Concept: Smart Mobility Indicator, Cybernetics, and Systems, 50(2), pp. 118-131, 2019.

[19] California Department of Transportation, Smart Mobility 2010: A Call to Action for the New Decade, Sacramento, State of California: California Department of Transportation, 2010.

[20] S. Šurdonja, T. Giuffrè, and A. Deluka-Tibljaš, Smart mobility solutions–necessary precondition for a well-functioning smart city, Transportation Research Procedia, 45, 2020.

[21] P. Berrone, and J. E. Ricart, IESE cities in motion index 2020. Publications Service of the University of Navarra, 2020.

[22] United Nations, Department of Economic and Social Affairs, Population Division, World Urbanization Prospects: The 2018 Revision, Online Edition, 2018.

[23] M. C. R. López, D. F. R. Melo, and Y. D. Wong, Transport barriers and its health implications in Asunción. Journal of Transport & Health, 14, 100579, 2019.

[24] C. A. Tovar, Latin American city, and present conflicts. Urban-Territorial Bitácora, 9 (1), pp. 64-8, 2005. Ciudad Latinoamericana y conflictos presentes. Bitácora Urbano-Territorial, 9(1), pp. 64-81, 2005.

[25] P. A. García, Qualitative research in the study of the relationships between daily mobility and poverty in the Latin American context: a case applied in metropolitan Lima. La investigación cualitativa en el estudio de las relaciones entre movilidad cotidiana y pobreza en el contexto latinoamericano: un caso aplicado en la Lima metropolitana, Documents d'anàlisi geogràfica, (55), pp. 57-76, 2009.

[26] I. Chaparro, Evaluation of the socioeconomic impact of urban transport in the city of Bogotá: the case of the Transmilenio mass transport system. ECLAC. Evaluación del impacto socioeconómico del transporte urbano en la ciudad de Bogotá: el caso del sistema de transporte masivo Transmilenio. CEPAL, 2002.

[27] L. S. Aparicio, The impact of transport on the organization of the city: the case of Transmilenio in Bogotá. Territories, (22), pp. 33-64, 2010. El impacto del transporte en el ordenamiento de la ciudad: el caso de Transmilenio en Bogotá. Territorios, (22), pp. 33-64, 2010.

[28] WHO. Data Bank, Mortality caused by road traffic injuries (per 100,000 people). Mortalidad provocada por lesiones por accidentes de tránsito (por cada 100.000 personas). [Online]. Available from: https://datos.bancomundial.org/indicator/SH.STA.TRAF.P5?most_recent_value_desc=false&view=map&year=2016 [retrieved: 03, 2021]

[29] R. Brandao, E. Diez-Roux, A. P. Taddia, S. M. De la Peña-Mendoza, and E. De la Peña, Road safety diagnosis in Latin America and the Caribbean: 2005-2009. Diagnóstico de seguridad vial en América Latina y El Caribe: 2005-2009. Inter-American Development Bank, 2013.

[30] WHO. 9 out of 10 people worldwide breathe polluted air, but more countries are taking action. [Online]. Available from: https://www.who.int/news-room/detail/02-05-2018-9-out-of-10-people-worldwide-breathe-polluted-air-but-more-countries-are-taking-action. [retrieved: 03, 2021]

[31] World Air Quality Report 2018. Published by Greenpeace and IQAir. [Online]. Available from: https://www.airvisual.com/world-most-polluted-cities/world-air-quality-report-2018-en.pdf. [retrieved: 03, 2021]

[32] L. Jaitman, Public Transport from a Gender Perspective: Insecurity and Victimization in Latin America, The Case of Lima and Asuncion Metropolitan Areas, Journal of Economics, Race, and Policy, 3(1), pp. 24-40, 2020.

[33] Numbeo. 2021. About Traffic Indices at This Website. Available from: https://www.numbeo.com/traffic/indices_explained.jsp [retrieved: 04, 2021]

 ISBN: 978-1-61208-863-1

Towards the Implementation of Ship Recognition and Identification System in Costal and River Information Services

Natalia Wawrzyniak
Marine Technology Ltd.
Szczecin, Poland
e-mail: n.wawrzyniak@marinetechnology.pl

Tomasz Hyla
West Pomeranian University of Technology
Szczecin, Poland
e-mail: thyla@zut.edu.pl

***Abstract*— The scope of the ship recognition and identification (SHREC) project covers development of three main system modules based on: detection and tracking, classification, and identification methods. First method allows to detect and track a moving ship while maintaining system performance, so it can be used to process data from multiple cameras (20 and more). Second method allows for classification of non-conventional ships into 5 to 7 classes using two Convolutional Neural Networks (CNN). This allows to recognize a type of ships when the identification is not possible. The identification method locates and recognizes hull inscriptions of detected units and matches them with records from available ships registers. Obtained information on ships can be automatically pushed into service oriented architecture of River Information Services (RIS) for alerting, statistics and authentication purposes. Currently, the integration and performance tests in marine and inland on-shore environment are close to finish. The obtained results imply that the SHREC is suitable for further integration with smart city services.**

Keywords- surveillance; ship identification; detection and tracking; river information services.

I. INTRODUCTION

Ships identification problems is addressed by many existing systems, as it is vital for safety and security of all on-water traffic participants and facilities on shore. Most solutions are directed in identifying large ship covered by Safety Of Life At Sea (SOLAS) [1] convention, which are oblige to use Automatic Identification System (AIS) transponders, have assigned unique International Maritime Organization (IMO) numbers, and have their hulls properly marked. The Ship Recognition and Identification System (SHREC) is being developed to automate the identification of non-conventional vessels in ports, harbors of both marine and inland waterways. It uses both traditional image processing and artificial intelligence methods (deep neural networks) to analyze video streams from existing monitoring systems as part of ship and port information systems.

In addition to the detection, classification and identification of units, the system's task is to transmit information about the ship to other system services and their recipients. This allows the information to be marked on electronic navigational charts and sent to interested services and authorities for notification, warning or statistical analysis.

The paper is organized as follows. Section 2 contains the description of three main modules of the system – detection and tracking, classification and identification. Section 3 summarizes the research emphasizing obtained results and pointing out some main constraints of the proposed solution.

II. GENERAL SYSTEM OVERVIEW

The system contains three main modules related to three main tasks of the system, together with an operator console module, the interfaces to the external systems, and a system core that contains systems logic that allows for interoperability between all mentioned parts. The core also stores the data and feeds the operator application with it. The system can use existing video monitoring system by capturing an analyzing its streams. These surveillance systems are usually part of vessel traffic information services implemented in critical water areas of moderate to heavy traffic or in proximity to crucial on-shore facilities. The services usually store or use information on ships coming from different hull registries of different kinds of vessels scattered in different authorities. SHREC system exchanges the data with such services by using it as reference data for ship identification purposes and sending back the information on detection, recognition or classification to RIS/VTS. For the communication with on-shore monitoring system 5G network is used together with a radio line set up between nodes further away from the city or port. Achieved results of systems main methods are presented below.

A. Detecting and Tracking

The method assumes that for each camera view there is a determined detection zone that eliminates areas of the scene where either ships cannot appear (e.g., on land) or they are too far for the detection process to make sense. The background subtraction algorithm is used for each frame from a video stream to obtain foreground objects, find their contours, and to obtain bounding boxes for each detected ship. The method is designed to detect all kinds of moving vessels and to work efficiently, so it can be used to process data from multiple cameras (20 or more) with usage of economically acceptable amount of server resources. The algorithm works in variable lightning conditions and with slight changes of the background. It detects water artefacts (by measuring number and length of edges). Furthermore, it identifies the same ship across the frames and is able to filter

 ISBN: 978-1-61208-863-1

out artifacts based on a 5 frame window. Exemplary scene is presented in Figure 1. Green frame shows a detected ship, yellow show places from 8 second were the ship was spotted, other colors show other objects (not ships) that were correctly rejected Movement direction is detected based on camera location. The HD resolution 1280x720 and GSOC background subtraction algorithm provide best results considering performance.

The method was tested using a test computer (Core i7-8700K, 32GB RAM, SSD 1TB, NVIDIA 311 Quadro P4000). The method returned around 90% of correct detection events for test sets of good quality scenes and around 80% for test sets of streams of bad quality. The incorrect detection events mainly arose from a few video samples with unfavourable lightning conditions. Some errors are corrected during later identification stage. More details can be found in [2].

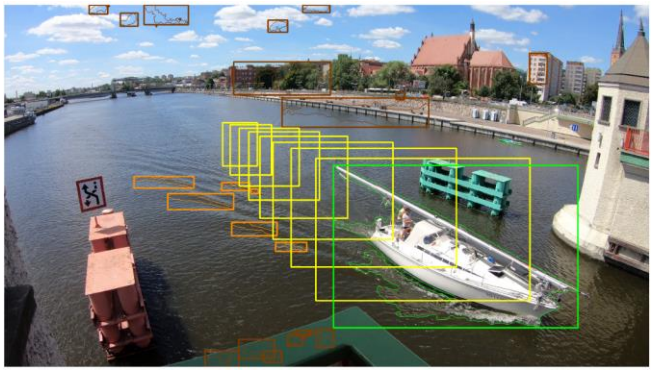

Figure 1. Detection method in action.

B. *Classification*

The module has two classification algorithms implemented. The first one is an implementation of the original CNN developed for the project, described in detail in [3]. Using only own-gathered data (recorded ships images) on 16 different architectures gave maximum ~20% efficiency during training. Training with the additional older database attached was ~41%. Finally, classification accuracy between 60 and 70% was achieved, but for only 5 classes.

For the purpose of achieving a proper classification quality, a second one was implemented using existing GoogleNet solution trained with thousands of images of non-SOLAS ships acquired during last 3 years the area cover by Lower Oder RIS System (Figure 2). The result that was achieved gave a classification accuracy of 84% for 7 classes (barge - together with pushed kit, motorboat, sailing yacht, kayak, service unit, passenger, and others). More information can be found in [4].

SHREC classification service can execute both classification algorithms at once. It also displays the last classified ship. Classification module is especially needed when identification is not possible due to unreadable vessel inscriptions.

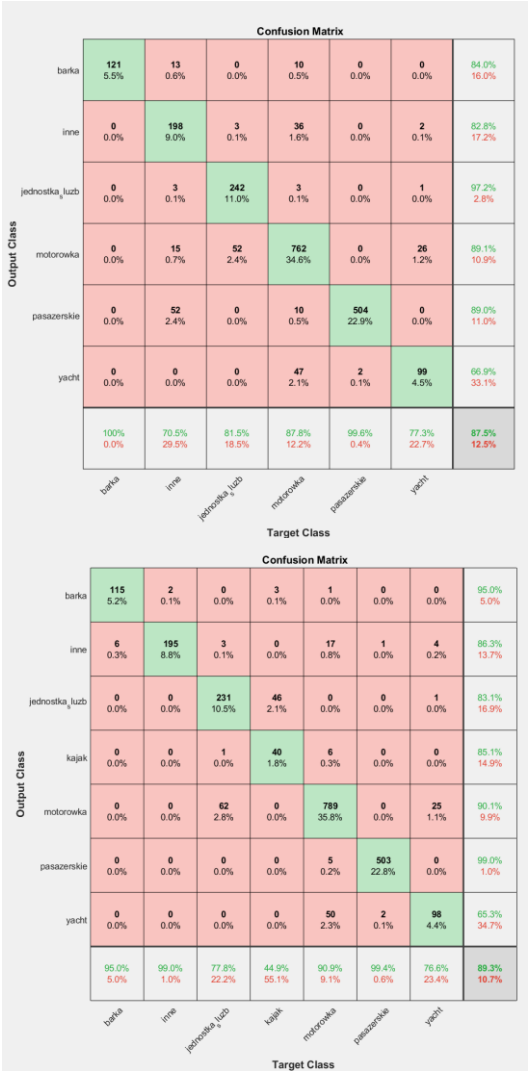

Figure 2. Exemplary confusion matrixes for different number of classes in pre-trained GoogleNet solution [4]

C. *Identification*

Vessel identification is based on the location and recognition of the hull inscriptions of the detected ship by the detection module. Our hybrid approach uses three text localization methods (CCA [5], MSER [6], EAST [7]) and Tesseract OCR to recognize inscriptions. The module uses its own ship registry (that can be fed from ships data bases from external services) and compares the found inscriptions with its records. It runs in near real time, in 5-second-rounds.

The degree of correct identification is determined depending on the degree of text matching. Conducted tests showed that the proposed method produced the 69% full matches of hull inscriptions (matched with no errors), 25% high matches (matched with one allowed error), 3% low matches (matched with two allowed errors), 3% multiple matches (matched simultaneously with more than one ship), and 9% of vessels were not identified. The methods architecture and tests were described in detail in [8].

 ISBN: 978-1-61208-863-1

The method works well identifying commercial vessels, as their inscriptions are placed according to the binding rules. With the recreational craft situation varies. When the visible inscription exceeds 10-12 pixels in height, the OCR returns satisfying results. Usually, the module analyses 10 to 20 vessels frames per vessel passage in front of the camera, while one with clear, visible characters is enough for proper recognition (identification).

III. SUMMARY

The tests results show that the system is able to recognize and identify all kids of ships using only video surveillances that are part of many already existing vessel monitoring systems. In a case when the identification is impossible, it classifies passing vessels into one of determined categories. The system detects vessels in less than a second with the background model updating 3 times per second during that process. Pre-identification is performed once per five-second round and the final identification outcome is given after the ships pass (after a round where tracking ID of the passing ship is lost). Deployment of proposed solution enables for automatization of operators work in monitoring centres and significantly reduces its cost. At the same time, it offers historical logs of identified and classified units and allows pushing statistics or alerting information to other services. This system is a smart management system for port and costal traffic services. The approach is in line with current trends for digitization, data sharing, and the development of the information society.

The main constrain of this solution is that the system is usable mainly in the daytime, in moderate to good weather conditions. Its operability is directly dependant on the quality of used cameras. A good night operability requires better than average hardware solution, such as CMOS sensors with low noise and suitable sensitivity, deliberated cameras placement, and the artificial source of light. Additionally, the classification module of the system was not trained using night-time ships' images as the traffic during night in summer months is very low and therefore, the classification accuracy during the night is unknown.

ACKNOWLEDGMENT

This work was supported by the National Centre for Research and Development (NCBR) of Poland under grant No. LIDER/17/0098/L-8/16/NCBR/2017.

REFERENCES

[1] IMO (1974) "SOLAS International Convention for the Safety of Life at Sea". International Maritime Organisation.

[2] N. Wawrzyniak, T. Hyla, and A. Popik, A. "Vessel Detection and Tracking Method Based on Video Surveillance". Sensors 2019, 19, 5230, pp 1-14

[3] M. Wlodarczyk-Sielicka and D. Polap,"Automatic Classification Using Machine Learning for Non-conventional Vessels on Inland Waters", Sensors, 2019, 19(14), 3051., pp 1-17

[4] K. Bobkowska and I. Bodus-Olkowska, "Potential and use of the GogleNet Ann for the purposes of Inland Water Ship Classification," Polish Maritime Research, vol. 4 (108), vol. 27, pp.170-178, 2020, doi:10.2478/pomr-2020–0077.

[5] S. Mule and S. N. Holambe, "Detecting Text in Natural Scenes with Connected Component Clustering and Nontext Filtering", IRJET, 2016, vol. 03(09), pp. 625-629.

[6] J. Matas, O. Chum, M. Urban, and T. Pajdla. "Robust Wide Baseline Stereo from Maximally Stable Extremal Region", in David Marshall and Paul L. Rosin, editors, Proceedings of the British Machine Conference, pp. 36.1-36.10, BMVA Press, September 2002, doi:10.5244/C.16.36.

[7] X. Zhou, et al., "EAST: An Efficient and Accurate Scene Text Detector". In Proceedings of the IEEE Conference on Computer Vision and Pattern Recognition (CVPR), Honolulu, HI, USA, 21–26 July 2017.

[8] T. Hyla and N.Wawrzyniak, "Identification of Vessels on Inland Waters Using Low-Quality Video Streams", Proceedings of the 54th Hawaii International Conference on System Sciences, 2021.

 ISBN: 978-1-61208-863-1

Current Situation of Smart Transport Component and a Strategic Overview Within The Scope of The Turkey's Smart City Maturity Assessment Model

H. Gülin Dizer
Department of Digital Strategy Development
TUBITAK BILGEM Research Institute for Software Technology
Ankara, Turkey
gulin.kocak@tubitak.gov.tr

Nuriye Ünlü
Institute Deputy Manager
TUBITAK BILGEM Research Institute for Software Technology
Ankara, Turkey
nuriye.unlu@tubitak.gov.tr

***Abstract*—This paper summarizes the capabilities and application of smart transportation component addressed within the scope of Smart City Maturity Assessment Model developed in the chaos of Turkish 2020-2023 National Smart City Strategy and Action Plan which is the 4th national smart city strategy in the world. There are many smart city maturity assessment models which enable cities to be evaluated together. In these models, standards and etc., different structures for different purposes are given over different concepts with different understandings. These found to be insufficient in terms of developing a national strategy by associating all smart city components under the smart city roof with each other. In addition, it has been determined that they do not meet the need to take into account the conditions and opportunities specific to Turkey. In this context, the need for Turkey-specific smart city maturity assessment model considering the current situation and future strategies of smart transportation component, which is defined in line with the Smart City Maturity Assessment Model, is emphasized. As a result, development of the Turkey specific maturity assessment model development and the Model itself became the backbone in analysis of the current situation and establishment of strategic view activities of the National Strategy and Action Plan.**

Keywords-smart transportation; smart cities; smart city maturity assessment model; maturity model; smart city components.

I. INTRODUCTION

There are many maturity assessment models that enable cities to feed each other and evaluate them together by comparing the smart city maturity of the cities in a systematic and structured way with a common understanding. When smart city maturity assessment models are examined, generally vertical assessment dimensions consisting of smart city components are used in models. As transportation services are the most used and needed service among city services, digitization in transportation services has become more important than other city services. In this context, many models such as [UNECE-ITU Smart and Sustainable City Indicators [1], Morgenstadt Framework Model [2], European Union (EU)-European Mid-Sized Cities Smart City Ranking Model [3], European Commission - Cultural and Creative City Monitoring Model [4] and ISO 37120 Sustainable Development of Communities-Indicators For City Services and Quality of Life, Smart Transportation, Smart Mobility and Logistics Management [5] are among the vertical dimensions mentioned in the evaluation of transportation services. These are evaluated in detail and found out that they have different structures with different concepts representing different understandings serving for different purposes. Moreover, they are evaluated as insufficient in terms associating all smart city components under the smart city roof with each other. At last, it has been determined that they do not meet the need to take into account the conditions and opportunities specific to Turkey.

With this approach, in Turkey within the scope of the 2020-2023 National Smart Cities Strategy and Action Plan [6] Project, Smart City Maturity Assessment Model [7] has been developed by TÜBİTAK BİLGEM Software Technologies Research Institute, which forms a common language and systematic structure guaranteeing simultaneous smart city maturity development. With the Model, the Smart City maturity level is determined by assessing smart city capabilities of a city and solutions are proposed for improvement of the maturity level. The developed model specific-to Turkey, is compatible with the country's current policy and takes sources and experience related to international examples into account.

The Smart City Maturity Assessment Model has been developed in the structure of displaying the current state of the city related to smart city transformation through status indicators, assessment of readiness in activity areas in division of competence-component-capability, and maturity level of efficiency dimensions, and display of the impact of smart city studies on the city through impact indicators. Smart City Capability is the skills that cities need / will need to perform smart city studies for a specific purpose or that they can / will acquire through smart city studies. Smart City Components are groups of capabilities that serve the same value. Smart City Competence is a group of consisting components based on sectorial expertise or service areas.

The Smart Transportation component is among the smart city components defined in the model. The existence of Smart Transportation applications in the cities, which are included in the breakdown of capabilities defined within the scope of the Smart Transportation component in the model, the state of intelligence creation based on the data and expertise obtained with these applications, and the use of this

 ISBN: 978-1-61208-863-1

intelligence in order to predict the improvement of the services provided by the use of these applications are evaluated. By determining the indicators used in measuring the current situation regarding smart transportation and the impact created by the smart city studies, the maturity level of the smart transportation component and its impact are evaluated.

There are four section in this paper. In first section, the case of addressing the smart transportation component to smart city maturity assessment models is described, the need for smart city maturity assessment model is evaluated, and, the structure of the model developed specific-to Turkey to meet this need is expressed. Section II describes the smart transportation component defined in scopes of 2020-2023 National Smart City Strategy and Action Plan Project and the Maturity Assessment Model work and the component capabilities and applications are included in this section. Section III provides information related to current state of smart transportation component in Turkey through the smart city maturity assessment model structure and the policies and indicators defined in this direction. In final section, the effects of studies to be conducted over the structure defined by developed model, on defined smart city policies are emphasized.

II. SMART TRANSPORTATION

The preparation studies of 2020-2023 National Smart Cities Strategy and Action Plan, analysis and examinations which adopted deductive and inductive approaches, were carried out in a way that feed each other and feed from each other iteratively and have become an integrated structure named Smart City Maturity Assessment Model. In smart city current state analysis studies, needs and problems were determined by

- focus group studies,
- strategy and legislation analysis,
- local government survey,
- examination of standards, framework models, sample applications developed both in Turkey and other countries.

With the knowledge conceptualization and modeling studies, capabilities and applications were defined within the scope of smart city components and components included in the maturity assessment model.

Among these components, the smart transportation component; developed for purposes such as reducing travel times, increasing traffic safety, optimum use of existing road capacities, increasing mobility, contributing to the national economy by providing energy efficiency and reducing the damage to the environment, is defined as sustainable integration of ICT-supported integrated systems, which include trams, buses, trains, subways, cars, bicycles and pedestrians using one or more modes of transportation, multi-directional data exchange between user-vehicle-infrastructure-center and monitoring, measurement, analysis and control, safe practices [6].

The capabilities identified within the scope of the smart transportation component are summarized below:

- Next generation vehicles: These are environmentally friendly vehicles with high fuel performance, low or no air pollutant emission.
- Next generation transportation models: These are models that adopt innovative approaches as well as the combined use of different transportation modes developed as an alternative to conventional transportation methods.
- Emergency management: It is the management of unexpected events that require emergency intervention in transportation.
- Accessibility management in transportation: It is the ease of people and commercial activities to reach the desired goods, facilities and activities in the transportation network.
- Transportation infrastructure: It consists of lines such as canals, waterways, airlines, railways and roads, as well as facilities such as terminals, ports, refueling depots, warehouses, bus stations, train stations and airports.
- Transportation governance: It consists of transportation planning, operation and maintenance, improvement and change management, continuity and integrated management.
- Logistics management: It is the supply chain management that provides the forward and backward flow of goods, services and related information between the production points and consumption points in line with the needs.
- Traffic management: It is the management of activities aimed at regulating urban traffic and ensuring its safety.
- Public transport management: Providing quality service for city residents using public transportation and managing vehicles and drivers in a holistic manner.
- Railway management: It is the management of the necessary activities for the safe and quality of railway safety and transportation.
- Park management: These are the activities required for the innovative, effective and efficient use of parking lots.
- Payment management: It is the establishment and management of the necessary infrastructures to make payment safe and easy in transportation.

The applications and application areas within the scope of smart transportation capabilities determined in line with the research conducted within the scope of model development activities are summarized in the following figure.

 ISBN: 978-1-61208-863-1

Figure 1. Capabilities and Applications of Smart Transportation Component.

As seen in Figure 1, within the scope of each smart transportation capability, the applications and application areas that cities should have in accordance with their smart city maturity levels are defined. Capability of next generation vehicles includes electric transportation vehicles, hybrid vehicles, autonomous vehicles, connected vehicles and capability of next generation transportation modes include car and bike sharing, multimode public transport, transport tunnels, demand responsive transport, multimode city transport traffic, targeted combination of different transport modes applications and etc. Capability of traffic management includes traffic intensity detector sensor, smart intersection solution center, real time and dynamic intersection management system, traffic measurement system, variable message system, intelligent guidance system, virtual twin and simulation in transportation, traffic light analysis, traffic analysis, trip planning, traffic jam assistant, lane warning system applications. Capability of public transport management includes smart stop, indoor mapping in transport, pedestrian access incentive implementation after public transport stops, common electronic ticket system in public transport, capability of

 ISBN: 978-1-61208-863-1

payment management includes city box office management, pricing for special cases, single card payment system applications. Parking management capability includes smart parking management and payment solutions, online parking reservation system, parking lot management and guidance system, vertical parking lots, park and use public transport system, parking lot dynamic pricing, parking lot occupancy applications. Railway management consists of train control system, railway safety monitoring system, railway infrastructure, intercity and high speed transport applications. Logistics management includes intelligent freight transport, special transport infrastructure for cargo systems, logistics data portal, freight mobility, logistics infrastructure applications. Accessibility in transport capability includes talking pedestrian button for disabled, personalized transportation information, pedestrianized zone, barrier-free accessible pedestrian routes, barrier-free traffic signaling, barrier-free public transport, standards for pedestrian roads and sidewalks. Capability of emergency management includes traffic light prioritization, emergency vehicle priority (evp) management, vehicle location detection, snow and ice fighting, preferential paths. And capability of transport governance includes data based transportation management, integrated traffic management, optimum route planning, traffic congestion based pricing, test evaluation center, traffic control center, urban network management, transport inventory database, passenger mobility , planning and implementation, operation and maintenance, monitoring evaluation and change management, sustainability, organization, resource management, service management, interoperability and coordination among stakeholders.

III. SMART TRANSPORTATION COMPONENT:CURRENT SITUATION AND STRATEGIC VIEW

Within the scope of 2020-2023 National Smart Cities Strategy and Action Plan [6] and Maturity Assessment Model [7] development studies, analyzing the current situation in terms of smart city components and defining expectations and solution suggestions for the future and identifying policies and strategies that will shape / affect the smart city area, the target view has been determined and a strategic perspective has been established. Within the scope of these studies, the Smart Transportation component has also been addressed.

The survey [8] conducted electronically by local governments is important in terms of determining the current status of smart transportation components in Turkey. 327 local governments (22 Metropolitan, 34 Provinces, 271 Districts) participated in the survey [8]. The structure of the smart transportation component in the smart city maturity assessment model was used in the questionnaire. An analysis was made with the answers given regarding the life cycle-based availability of 41 applications within the scope of the Smart Transportation component.

As part of the local government survey [8], in the area of smart transportation;

- 7% of cities have “Next Generation Vehicle and Transportation Modes” capability,
- 8,9% of cities have “Smart Traffic Managements” capability,
- 5,5% of cities have “Smart Parking” capability,
- 12,7% of cities have “Accessibility in Transportation” capability,
- 7,5% of cities have “Emergency Management” capability,
- 6,6% of cities have “İnfrastructure Management, Public Transport Management, Payment Management, Railway Management, Transportation Governance and Logistic Management” capabilities

have been found that the foregoing considerations exist at different stages of the life cycle. Thus;

- 8% of cities have “Electric vehicles/Buses” applications,
- 4% of cities have “Hybrid vehicles” applications,
- 9% of cities have the “Maintenance Repair Assistance” applications
- 7% of cities have “Parking Assistance” applications,
- 5% of cities have “Traffic Jam Assistance” applications,
- 4% of cities have “Vehicle Sharing” applications,
- 10% of cities have “Bike Sharing” applications,
- 7% of cities have “Multi-Mode Public Transport” applications,
- 5% of cities have “Emergency Change Management” applications
- 10% of cities have “Traffic Light Prioritization” applications,
- 5% of cities have “Vehicle Priority Management” applications,
- 11% of cities have " Talking Pedestrian Buttons for Disabled Persons” applications,
- 5% of cities have “Personalized Transportation Information” applications,
- 22% of cities have “Pedestrianized Zone” applications,
- 1% of cities have “Smart Vehicle Highway Systems” applications,
- 4% of cities have “Lane Warning System” applications,
- 5% of cities have “Lane Management Arrangement” applications,
- 5% of cities have “Car Park Dynamic Pricing” applications,
- 8% of cities have “Car Park Occupancy Determination” applications,
- 7% of cities have “Parking Management and Routing System” applications,
- 2% of cities have “Online Parking Reservation System” applications,
- 4% of cities have “Intensity Density Sensors” applications,
- 6% of cities have “Smart Solution Center” applications,

 ISBN: 978-1-61208-863-1

- 8% of all cities have “Real-time and Dynamic Junction Management Systems” applications,
- 8% of all cities have “Light Analyses” applications,
- 14% of cities have of “High Speed Transport” applications,
- 8% of cities have “Commuting to Work and Regional Transportation” applications,
- 7% of cities have “Trip Planning” applications,
- 5% of cities have “Demand Based Transportation” applications,
- 1% of cities have “Traffic Jam Based Pricing” applications,
- 9% of cities have “Traffic Analyses” applications,
- 4% of cities have “City Ticket Office Management” applications,
- 12% of cities have “Determination of Vehicle Routes with GPRS Data” applications,
- 7% of cities have “Smart Routing Center” applications,
- 13 % of cities have “Traffic Monitoring System” applications,
- 9% of cities have “Traffic Measurement System” applications,
- 9% of cities have “Traffic Violation Systems” applications,
- 8% of cities have “Variable Messaging System” applications,
- 5% of cities have “Integrated Traffic Management” applications,
- 2% of cities have “Connected Traffic Cloud” applications,
- 9% of cities have “Urban Traffic Management Systems” applications

have been found that the foregoing considerations exist at different stages of the life cycle.

In this context, policies developed are as follows:

- The need to evaluate the use of the next generation efficient and low carbon release vehicles, a next generation transportation models and reduced traffic and increased user comfort has been determined as a policy area. The dissemination of new generation environmentally friendly (with alternative power system) means of transportation will be ensured. In addition to the combined use of different transportation modes developed as an alternative to classical transportation methods, the widespread use of next-generation transportation models addressing innovative approaches will be ensured.
- The need for efficient management of traffic based on data, optimizing the time spent in traffic, facilitating the lives of city residents and providing safe travel has been determined as a policy area. In this context, there is a need to improve the transportation infrastructure and expand the application / application areas within the scope of transport infrastructure, public transport management, railway management, payment management, parking management and governance capabilities.
- There is a need to develop transportation infrastructure and extend applications/application areas. Infrastructure that supports smart transportation systems will be deployed.
- There is a need to develop transportation infrastructure and extend applications/application areas. Activities intended for transportation governance will be conducted at the national, regional and local level for organization, resource management, planning and implementation, operational maintenance, monitoring evaluation, sustainability, interoperability, service management and coordination among stakeholders.
- In smart transportation area, it is needed to provide emergency transportation management and provide transportation without interruption by vehicle priority in case of emergency and disasters. Within the scope of emergency transportation management, the widespread use of information systems that provide traffic light routing and automatic detection of cases will be ensured in order to provide the rapid transportation of priority vehicles in traffic as required.
- There is a need for talking pedestrian buttons for disabled people, unobstructed pedestrian paths, unobstructed accessible traffic signalization and the use of personalized transportation information through unobstructed accessible public transportation applications to ensure accessibility in transportation. To ensure accessibility in transit, all segments on the transportation network will be foreseen for smooth and easy use, as well as advance notification of transportation options and widespread use of applications for disabled people.
- By building a Smart haulage infrastructure, the development of the logistics data portal and the provision of logistics management are required. Data-driven logistics management will be undertaken, based on needs that embraces the generation supply chains that provide forward and reverse flows of goods, services and related information between production point and consumption points.
- There is a need to provide inclusive transport services that improve the quality of life of city residents and ensure safe mobility of drivers, pedestrians and passengers.

The indicators determined in order to measure the effect of the policies developed for the smart transportation component on the current situation are as follows:

- Status Indicators
  - The number of public transport trips per person per year
  - The number of personal cars per person
  - Percentage of people who use a travel mode other than a personal vehicle
  - The number of vehicles with two wheels per person

 ISBN: 978-1-61208-863-1

    - Percentage of cycle paths and lanes per 100000 people
    - The number of deaths in transportation per 100000 people
    - Real-time traffic information presentation rate
    - Measurement status of the amount of renewable energy used in transportation
    - Existence of the physical infrastructure provided for the sharing of electric vehicles
- Impact Indicators
    - The number of cities with increasing Smart Transportation Maturity of the Component
    - National Smart Transportation maturity level increasing status
    - Increasing status for the length of the high capacity public transportation system per 100000 people
    - Increasing status for of the length of the light passenger public transportation system per 100000 people
    - Increasing status for commercial air connection (the number of continuous commercial air destinations)
    - Increasing status of the amount of renewable energy used in transportation.

IV. CONCLUSION

Since the smart city is a complex concept, it is necessary to give a structure for the concept. Smart city maturity assessment models are used to meet this need. With this approach, Turkey specific maturity assessment model has been developed and the model have been used in analysis of the current situation and establishment of strategic view activities within the scope of the National Strategy and Action Plan development. In this context, the current situation was determined in a structural, related and systematic way through the architecture of the model defined and the strategies, namely the target view, were expressed over the same structure. Within the scope of the model, the smart transportation component, its capabilities and applications were determined and the needs definition studies and target view determination studies for the smart transportation component were shaped through this structure.

To summarize, for the future the implementation of adopted policies will be ensured by measuring the development and impact of the smart city studies carried out in the city with city-based model implementation. On the other hand, new solutions are constantly added to smart transportation solutions, and some of them are not preferred because they do not create the desired value in practice. Therefore, it is necessary to reflect these changes to the model continuously, and there is a need to address such a large number of city-based solutions in line with the priorities defined in the city smart city strategy (possibility, condition, need and current smart transportation maturity).

ACKNOWLEDGMENT

The authors would like to thank Institute Manager of TUBİTAK BILGEM YTE Cemil Sağıroğlu, Gizem Kabayel, Mavişe Dilek, Çağatay Yamak, M. Eren Akbaş, Mürüvvet Ünal Byram and Muhammed Ali Güntay for their help and support in making this work possible.

REFERENCES

[1] UNECE/ITU. Smart Sustainable Cities Indicators. [Online]. Available from: http://www.unece.org/fileadmin/DAM/hlm/projects/SMART_CITIES/ECE_HBP_2015_4.pdf 2021.02.26

[2] Fraunhofer. Morgenstadt Framework. [Online]. Available from: https://www.researchgate.net/profile/Alanus-Radecki/publication/283319948_The_Morgenstadt_Framework/links/5633275808ae242468daa422/The-Morgenstadt-Framework.pdf 2021.02.26

[3] European Union. European Initiative on Smart Cities. [Online]. Available from: https://setis.ec.europa.eu/set-plan-implementation/technology-roadmaps/european-initiative-smart-cities 2021.02.26

[4] European Commission. The Cultural and Creative Cities Monitor Joint Research Centre 2017 Edition. [Online]. Available from: http://publications.jrc.ec.europa.eu/repository/bitstream/JRC107331/kj0218783enn.pdf 2021.02.26

[5] ISO. 37120 Sustainable Development of Communities -- Indicators For City Services and Quality of Life.[Online]. Available from: https://bsol.bsigroup.com/ 2021.02.26

[6] Republic of Turkey Ministery of Enviroment and Urbanisation. 2020-2023 National Smart Cities Strategy and Action Plan. [Online]. Available from: https://www.akillisehirler.gov.tr/wp-content/uploads/EylemPlani.pdf 2021.02.26

[7] TUBITAK BILGEM YTE. 2020-2023 National Smart Cities Strategy and Action Plan Smart City Maturity Assessment Model. Project Document 2018.07.13

[8] TUBITAK BILGEM YTE. 2020-2023 National Smart Cities Strategy and Action Plan Project, Local Government Survey.-2019. Project Document 2018.07.13

 ISBN: 978-1-61208-863-1

Development of New generation Low-Cost Conductivity System for Crop Irrigation Monitoring

Daniel A. Basterrechea, Sandra Sendra, Sandra Viciano-Tudela, Jaime Lloret
Instituto de Investigación para la Gestión Integrada de Zonas Costeras,
Universitat Politècnica de València.
Gandía, Valencia (Spain)
Email: dabasche@epsg.upv.es, sansenco@upv.es, sandraviciano8493@gmail.com, jlloret@dcom.upv.es

***Abstract*—The development of smart cities has been boosted in recent years. This means improvements for urban agriculture. In this paper, we present a low-cost system for monitoring conductivity in the irrigation system of urban agricultural plots. For this purpose, an inductive, two-coil sensor has been developed, where one is located inside the other. For the experiment, we have used three prototypes with 40 spires for the fed part and 80 spires for the induced part, but with different pipe diameters. P1 has 20mm, P2 25 mm, and P3 32 mm. The sensors were calibrated using salt between 0 g/L and 20 g/L concentrations. We use concentration of 0 g/L, 2.5 g/L, 5 g/L, 10 g/L, 15 g/L and 20 g/L with conductivity of 0.485mS/cm, 5.53 mS/cm, 10.43 mS/cm, 20.4 mS/cm, 31.3 mS/cm, and 41.6 mS/cm. The voltage difference between the minimum and maximum concentrations in each prototype is 1.71 V for P1, 1.41 V for P2, and 0.99 V for P3. Subsequently, the verification of each prototype was performed, measuring concentrations of 7.5 g/L, 12.5 g/L, and 17 g/L, obtaining the lowest relative errors for P1 and P3 with 0.34% and 0.31% respectively.**

Keywords—Conductivity sensor; urban agriculture; irrigation monitoring.

I. INTRODUCTION

For the first time, more than half of the population lives in cities. Villages or small towns are being depopulated and more are living in cities. Due to the rural exodus, food production is becoming complicated and expensive. This situation is most relevant in developing countries, where people with limited economic resources have difficulty accessing basic foodstuffs [1].

In this situation, the smart cities (SM) concept has begun to take on great relevance [2]. SM integrates new technologies with traditional infrastructures. This synergy improves the operational and management functions of the city, increases control, and optimizes the resources of the city itself. In this context, Urban Agriculture (UA) starts to gain relevance [3]. This type of practice is carried out on relatively small plots of land and is used for the self-sufficiency of certain groups within cities. This type of agriculture reduces the carbon footprint by reducing the transport of the products obtained from the fields to the cities. Conversely, due to water resource management, many urban farmers use untreated municipal wastewater as irrigation water [4]. This can cause crop damage.

At present, the most widely used methods for controlling the quality of irrigation water are sampling and subsequent laboratory analysis. This process has several disadvantages, such as the need to have a person to take the sample, the need to have a laboratory and the waiting time for the analysis to be carried out, making it an inefficient process. One of the most relevant parameters for detecting changes in water quality is conductivity [5]. Conductivity is considered an indicator of water quality, because it displays the purity of the water or whether it contains dissolved chemicals or minerals. In this context, a high load of dissolved substances would show a high conductivity, which is harmful to the crop. Furthermore, in recent years, alternatives have emerged to monitor the quality of irrigation water. These methods are expensive or do not allow continuous monitoring in different parts of the irrigation pipes, being systems that are difficult to apply in environments such as urban plots.

In this paper, we propose the development of a low-cost system for conductivity monitoring of irrigation water used for urban agriculture. The sensor used in this system is based on the same principle as previously developed sensors [6], based on the generation of electromagnetic fields, which interact with the medium causing changes in it. The current prototype is considered progress as the design used adapts more optimally to irrigation pipes, where previous developments could not. The prototype developed has a central coil and a shallow coil around the pipe, causing minimal obstruction to the internal flow of water in the pipe.

The rest of the paper is structured as: Related works are presented in Section II. Then, the Test Bench is presented in Section III. Section IV shows the proposal performed. Then, the results are shown in Section V. Finally, the conclusion is presented in Section VI.

II. RELATED WORK

In this section, we show the different works carried out, and explain the advantages of our system compared to others.

N. A. Cloete et al. [7] proposed the design and development of a water quality monitoring system. The objective of this system is to notify the user of the real-time water quality parameters. This system is able to measure flow, temperature, pH, conductivity, and oxidation-reduction potential. They use ZigBee receiver and transmitter modules for communication. The proposed system is capable of reading physiochemical parameters, and can successfully process, transmit, and display the readings. Then, N. Vijayakumar [8], present a design and development of a low-cost system for real-time monitoring of the water quality in IoT (internet of things). This system measures different parameters like temperature, PH, turbidity, conductivity, dissolved oxygen. Moreover, they proposed the use of PI B+ model as the core controller. In the same context, F. Anthony et al [9] developed Water Sensor Network (WSN) system prototype developed for water quality monitoring in Victoria Basin (LVB). This system uses an Arduino microcontroller, water quality

 ISBN: 978-1-61208-863-1

sensors, and a wireless network connection module. The parameters that are able to measure are temperature, dissolved oxygen, pH, and electrical conductivity in real-time and disseminates the information in graphical and tabular formats to relevant stakeholders through a web-based portal and mobile phone platforms.

W. Gong et al. [10] proposed a conductivity sensor based on two flat electrodes built on a PBC board. For the measurements, they use KCI and water MQ. The sensor is suitable for marine environments. This sensor works at 334kHz obtaining significant variations in a wide range of salinity. Then, J. Zang et al [11] proposed a new four-electrode smart sensor for water conductivity measurements of aquaculture monitoring. This sensor has high precision with good stability. This system includes a temperature sensor to compensate for the water conductivity temperature dependence. The developed conductivity is appropriate for measuring conductivities between the range of 0-50 mS/cm, 0-40ºC.

Besides, J. Rocher et al [12] proposed a system for detecting illegal dumping. The proposed system is based on a conductivity sensor. This sensor is composed of two coils. One of the coils is powered by a sinus-wave and the other coil is induced. They experiment in a laboratory where the selected prototype has an 4.10 Volts between the samples 0 and 40 g/l of the table salt. Then D.A. Basterrechea et al [13] presents a test of three prototypes with different characteristics for controlling the quantity of organic fertiliser in the agricultural irrigation system. They perform the test using six samples between the 0 g/L and 20 g/L of organic fertiliser and measure their conductivity. They obtained that in prototype 1 (P1) (coil with 8 layers) the working frequency is around 100 kHz, in P2 (coil with 4 layers) around 110 kHz, and for P3 (coil with 2 layers) around 140 kHz. Finally, the results displayed that prototype three with configuration 1 is the best device to be used as a fertiliser sensor in water.

Currently, the coil designs produced are not adaptable to irrigation pipes, as these have been designed for wider spaces. Therefore, the new generation of coils developed is suitable for use in different pipe diameters.

III. TEST BENCH

In this section, we present the prototypes that have been used and the experiments that have been carried out with each group of sensors. In addition, the test bench is made up of two subsections.

A. Prototype characterization

For this experiment, we have created different prototypes for the agricultural irrigation system. These new prototypes, unlike the previous ones, can be installed in the irrigation pipes with the minimum possible interruption in the water flow. Moreover, they can be adapted to different pipe diameters. In addition, PVC of different diameters for the fed coil, such as 20 mm for P1, 25 mm for P2, and 32 mm for P3, has been used for the construction of these new prototypes. The length of the sensors used is 7.5 cm, with a thickness of 2 mm. The induced coil is placed inside the PVC pipe. For this second coil, a polyethylene (PE) pen sleeve filled with silicone has been used to create a solid core, which measures 5.3 cm. The diameter of the second reel is also 7mm. A ratio of 40 coils for the power supply (PC) on the external side and 80 coils for the induction coil (IC) on the internal side has been used.

The three prototypes developed are shown in Figure 1 where they are compared with prototype designs from previous research. The current prototype has a coil on the external side of the pipe. In comparison to the previous ones, these are suitable to be placed in the pipes directly.

B. Performance of the experiment

In order to perform our experiments, the following parameters have been selected (see Table I).

TABLE I. SELECTED PARAMETERS FOR THE EXPERIMENT.

	Parameters
Tested Frequencies	450-520 Khz
Type of water	Drinking water
Temperature	25C^{o}
NaCl concentration range	0 g/L-20 g/L

For the experiment, we started by placing two PVC elbows on each pipe to simulate real pipe conditions. In addition, we added a specific volume to each sensor. These added volumes are the ones required to cover the pipe completely. Furthermore, for P1 we used 105 mL of, 60 mL for P2, and 30 mL in P3. Once the pipe was filled, each prototype was connected one by one to the generator and oscilloscope. In this case, the supplied coil was connected to the AFG1022 generator [14] with a 3.3 V peak-to-peak supply generating a sinusoidal signal. Besides, the induced coil was connected to the TBS1104 oscilloscope.

Following the connection of the sensor, we perform a frequency scan to determine the frequency where the magnetic field generated by the sensor is most sensitive to the medium. This frequency is considered the working frequency. Once the working frequency has been obtained, we begin to take data. To do this, values are taken using 6 solutions of different NaCl concentrations. These concentrations are 0 g/L, 2.5 g/L, 5 g/L, 10 g/L, 15 g/L and 20 g/L. The conductivity is measured with a Basic-30. The conductivity values obtained are 0.485mS/cm, 5.53 mS/cm, 10.43 mS/cm, 20.4 mS/cm, 31.3 mS/cm, and 41.6 mS/cm. Triplicate values are taken and then averaged. The most stable value displayed by the oscilloscope is chosen for measurement. After taking the measurements, the calibration curve is made to determine the correlation of the values obtained with the salt concentration. Finally, verification was carried out using solutions of 7.5 g/L, 12.5 g/L, and 17 g/L, which were measured obtaining a conductivity of 15.45 mS/cm, 26.3 mS/cm, and 36.8 mS/cm.

IV. PROPOSAL

This section presents the design and test of the power circuit to generate the sinusoidal signal to power the water presence sensor.

A. ICM7555 circuit.

In order to power the different prototypes of the coil, it is required a power supply and excitation circuit to generate an alternating current similar to sinusoidal signals. To do this, a 555 series oscillator integrated circuit can be used. This circuit is configurable by using different values of resistors and capacitors. Figure 2 shows the schematic of the 555 modules in astable mode and the recommended equations for calculating the generated frequency.

 ISBN: 978-1-61208-863-1

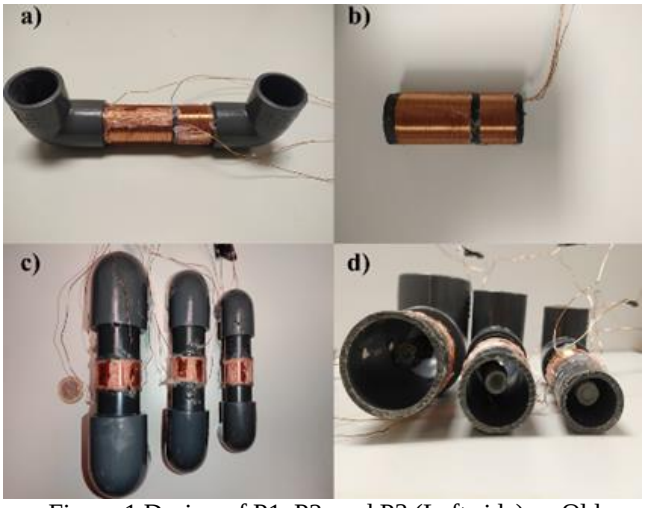

Figure 1.Design of P1, P2, and P3 (Left side) vs Older sensor (Right side).

For configuring a duty cycle of 50%, it is recommended to use the values of RA = 1 kΩ and RB = 10 kΩ. As we will see in the next section, the three prototypes we use present a working frequency between 460 kHz and 470 kHz. So, the value of C should also be determined. Using the recommended equations, we have calculated the theoretical value of C to obtain those frequencies. However, checking the actual functioning of this circuit, some differences are observed (see Table II). These differences can be due to the tolerances of all components.

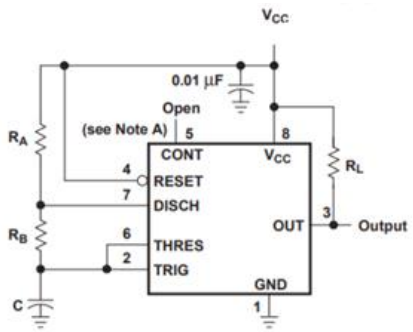

$$f \approx \frac{1.44}{(R_A + 2R_B)C} \quad (Hz)$$

$$D = \frac{R_A + R_B}{R_A + 2R_B} \cdot 100 \quad (\%)$$

Figure 2. *555 modules in astable mode and equations to determine the frequency and duty cycle.*

TABLE I. VALUES OF C FOR OBTAINING THE DESIRED FREQUENCIES

Value	C_{real}	F_{theo}	F_{real}
1	140pF	481kHz	360.6kHz
2	80pF	861kHz	468.9kHz
3	40pF	1.72MHz	505kHz

B. *Design of power circuit*

The power circuit is in charge of powering the primary coil. As we mentioned before, it is based on the ICM7555 in the astable configuration. The output voltage provided by this circuit is too low for the power of the primary coil, so, we included an NPN transistor. This component is in charge of allowing the circulating of current to the primary coil located in parallel with a resistor. The resistor placed on the collector of the NPN transistor is used to limit the current that drives through it. A diode in a flyback configuration prevents that a continuous current circulates in the coil causing the coil to become in a short-cut. The transistor will invert the sense of current through the resistor and the coil will begin to discharge until a new cycle. All these components compose the amplifier phase. In this part of the circuit, there is no AC signal. However, there is a change in the current sense, so a current is induced on the secondary coil that will help us to detect the presence of water in the pipe. Finally, it is included a Double wave rectifier bridge followed by an RC filter. Those elements are used to obtain a DC valued proportionally to the presence of water in the pipe. The circuit implemented is shown in Figure 3.

V. RESULTS

This section represents the results of the different prototypes developed and the comparison of these with prototypes made in other studies.

A. *Old prototypes*

Figure 4 shows the results obtained with the previous prototypes when applying them outside the pipe. The values obtained are homogeneous in 9.28 V at its working frequency of 210 kHz. The calibration curve reflects the fact that there is no difference between the different concentrations of salt solutions used.

B. *Current prototypes*

Figure 5 shows the frequency sweep carried out for the 3 different prototypes developed. It can be seen that the sweep frequencies performed are in a similar range for P1, P2, and P3, since the same proportion of spires has been used in both the PC and IC parts. The results obtained show that the frequencies where the voltage is higher are 480 kHz for P1 and 490 kHz for P2 and P3.

Once the frequency sweep has been carried out, measurements are taken at each of the frequencies previously displayed for different concentrations of salinity. These concentrations are in the range of 0 g/L and 20 g/L. The results obtained provide the WF of each prototype which is detailed in Table III. The WF of prototypes 1 and 2 is 470 kHz and of the P3 460 kHz. In addition, the highest voltage change is found at P1 with 1.71 V.

TABLE II. WF OF P1, P2, AND P3 WITH THEIR RESPECTIVE VOLTAGE DIFFERENCES BETWEEN THE LOWEST AND HIGHEST SALT CONCENTRATION

Prototypes	Vout (difference)	WF
1	1.71	470
2	1.41	470
3	0.99	460

 ISBN: 978-1-61208-863-1

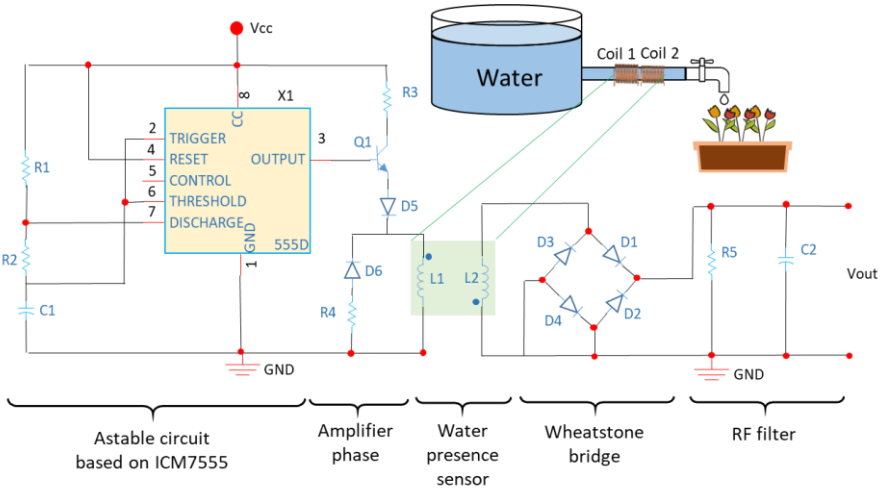

Figure 3. Power circuit schematic.

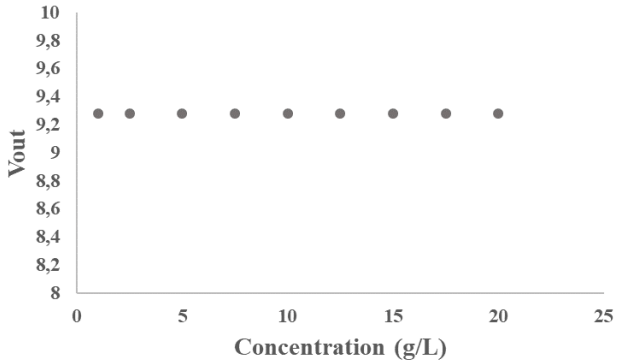

Figure. 4. Calibration of the old prototype for different NaCl concentrations.

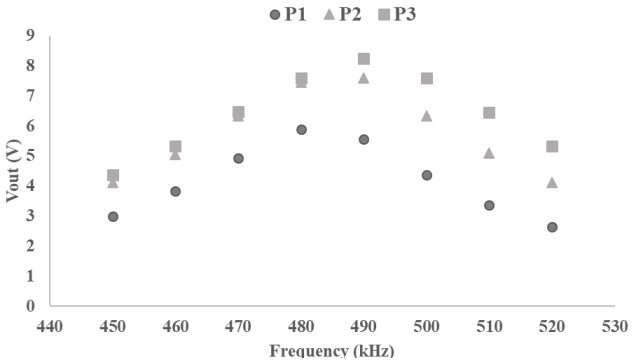

Figure 5. P1, P2, and P3 frequency sweep.

The calibration of each prototype for these frequencies was carried out once the WF was obtained, using 6 different concentrations from 0 g/L to 20 g/L every 2.5 g/L. Figure 6 represents the calibration lines for P1, P2 and P3. This represents a minimum voltage of 4.92 V and a maximum voltage of 6.63 V for P1. The change presented is about 1.71 V. The maximum changes between the measured points are located in the first 3 points, then the values stabilise. The highest variation is presented between the concentration of 0 g/L and 2.5 mg/L with 0.56 V.

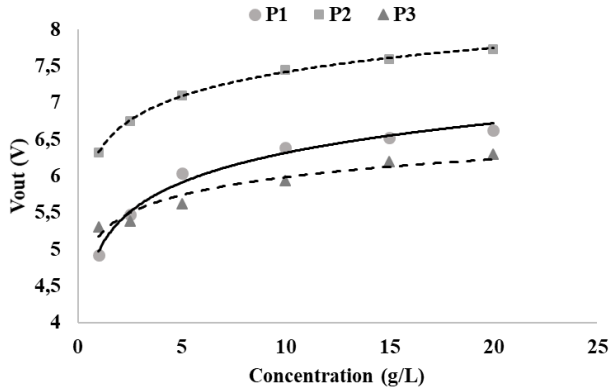

Figure 6. Calibration model of P1, P2 and P3.

Similarly, P2 shows a minimum and maximum voltage of 6.32 V and 7.73 V, with a voltage change of 1.41 V. The maximum changes between the measured points are located in the first 3 points, then the values stabilise. The highest variation is 0.42 V, presented between concentrations of 0 g/L and 2.5 mg/L.

Finally, the calibration model of P3 presented the values for the lowest concentration of 5.3 V and for the highest concentration of 6.29 V. The maximum change between these two concentrations is 0.99 V. The highest variation is presented between the concentration of 0 g/L and 2.5 mg/L with 0.24 V.

The calibration curves obtained for each of the prototypes offer a determination coefficient (R^2) whose main purpose is to predict future results or test a hypothesis. In this context, the highest R2 is found in P1 with a value of 0.9848. Then we find P2 with 0.9834 and P3 with 0.9367. The equations of each prototype are given by (1)-(3). In addition, the three prototypes present a logarithmic adjustment of the obtained values.

$$Vout = 0.5822 * \ln(Concentration(g/L)) + 4.9741 \quad (1)$$

$$Vout = 0.3960.* \ln(Concentration(g/L)) + 6.3737 \quad (2)$$

$$Vout = 0.3516 * \ln(Concentration(g/L)) + 5.1739 \quad (3)$$

C. Verification

Finally, a verification of the developed prototypes was carried out. For this purpose, 3 salt solutions of 7.5 g/L, 12.5 g/L, and 17.5 g/L were used. Table II shows the results obtained for each of the prototypes. The errors presented in the table have been obtained on an absolute value basis. Furthermore, the results show that P3 and P2 have the lowest errors, with an Absolute Error (AE) of 0.01 V and

0.02 V, and a Relative Error (RE) of 0.31 % and 0.34 % respectively. On the other hand, P2 is the one that displays the highest error with 0.13 V of AE and 1.79 % for ER.

TABLE III. VERIFICATION OF THE P1, P2, AND P3.

NaCl. (g/L)	P1		P2		P3	
	AE (Vout)	*RE (%)*	*AE (Vout)*	*RE (%)*	*AE (Vout)*	*RE (%)*
7,5	0,08	1,28	0,15	2,03	0,16	2,84
12,5	0,04	0,55	0,11	1,42	0,06	0,95
17,5	0,05	0,82	0,15	1,91	0,06	0,96
Average	0,02	0,34	0,13	1,79	0,01	0,31

In this context, we discarded P2 due to its high error compared to the others. Similarly, although P3 shows a lower error than P1, the last one is chosen as the best option for water monitoring in the irrigation system of urban agriculture. This is because P1 displays higher voltage differences between the minimum and maximum salt concentration, being 1.71 V for it versus 0.99 V for P3.

VI. CONCLUSION

Water quality monitoring in urban agriculture is of great importance to improve and optimise production from these gardens. In addition, conductivity can be classified as one of the most important parameters for detecting changes in the quality of the irrigation water used.

In this paper, we proposed a new generation low-cost system for monitoring the irrigation of urban crops. The presented sensor is optimally adapted to the irrigation pipes with minor influence on the water flow. We have determined the working frequency of the different prototypes with common salt (NaCl). The results indicate an optimal behaviour of the 3 prototypes, being the P1 the best option. This last prototype has the highest voltage difference between the minimum and maximum concentrations. In addition, the relative error is one of the smallest values of the test.

In future work, we want to improve the sensitivity of our sensor and different salts, suspended solids and pre-treated waster waters. Since it is possible to have pipes of not only PVC but also concrete and metals alloys, we would also test our system in those type of pipes and investigate the possibility of integrating them in the manufacturing of concrete coils. Finally, we will test the developed sensor in a real environment, taking measurements in a dynamic system.

ACKNOWLEDGMENT

This work has been partially supported by the European Union through the ERANETMED (Euromediterranean Cooperation through ERANET joint activities and beyond) project 41-227 SMARTWATIR.

REFERENCES

[1] F. Orsini, R. Kahane, R. Nono-Womdim and G. Gianquinto, “Urban agriculture in the developing world: a review”, *Agronomy for sustainable development* , vol. 33, no 4, pp. 695-720, May 2013, https://doi.org/10.1007/s13593-013-0143-z

[2] M. Batty et al., “Smart cities of the future”, The European Physical Journal Special Topics, vol. 214, no 1, pp. 481-518, December 2012, https://doi.org/10.1140/epjst/e2012-01703-3

[3] M. N., Poulsen, P. R. McNab, M. L. Clayton and R. A. Neff, “Sytematic review of urban agriculture and food security impacts in low-income countries”, Food Policy, vol. 55, pp. 131-146, August 2015, doi: https://doi.org/10.1016/j.foodpol.2015.07.002

[4] Food and Agriculture Organization (FAO). Water agriculture. [Online]. Available from: http://www.fao.org/fcit/upa/water-urban-agriculture/es/. [retrieved: April, 2021]

[5] T. A. Bauder, R. M. Waskom, P. L. Sutherland, and J. G. Davis. Irrigation water quality criteria. Colorado State University: doctoral thesis, 2011.

[6] J. Rocher, D. A. Basterrechea, L. Parra and J. Lloret, “New Conductivity Sensor for Monitoring the Fertigation in Smart Irrigation Systems”, International Symposium on Ambient Intelligence. Springer, Cham, June 2019, pp. 136-144, doi: https://doi.org/10.1007/978-3-030-24097-4_17.

[7] N. A. Cloete, R. Malekian and L. Nair, “Design of smart sensors for real-time water quality monitoring”, IEEE access, vol. 4, p. 3975-3990, July 2016, doi: 10.1109/ACCESS.2016.2592958.

[8] N. Vijayakumar and A. R. Ramya, “The real-time monitoring of water quality in IoT environment”, International Conference on Innovations in Information, Embedded and Communication Systems (ICIIECS), IEEE, March 2015, pp. 1-5, doi: 10.1109/ICIIECS.2015.7193080.

[9] G. Eason, B. Noble and I. N. Sneddon “On certain integrals of Lipschitz-Hankel type involving products of Bessel functions,” Phil. Trans. Roy. Soc. London, vol. A247, pp. 529–551, April 1955, doi: https://doi.org/10.1098/rsta.1955.0005.

[10] W. Gong, M. Mowlem, M. Kraft and H. Morgan, “Oceanographic sensor for in-situ temperature and conductivity monitoring”, Oceans 2008-Mts/IEEE Kobe Techno-Ocean (OTO’08), May 2008. pp. 1-6, doi: 10.1109/OCEANSKOBE.2008.4530906.

[11] J. Zhang, D. Li, C. Wang and Q. Ding, “An intelligent four-electrode conductivity sensor for aquaculture”, International Conference on Computer and Computing Technologies in Agriculture”, Springer, Berlin, Heidelberg, 2012, pp. 398-407, doi: https://doi.org/10.1007/978-3-642-36124-1_48

[12] J. Rocher, D. A. Basterrechea, M.Taha, M. Parra and , J. Lloret, “Water Conductivity Sensor based on Coils to Detect Illegal Dumpings in Smart Cities” Fourth International Conference on Fog and Mobile Edge Computing (FMEC). IEEE, June 2019. pp. 324-329, doi: 10.1109/FMEC.2019.8795341.

[13] D. A. Basterrechea, L. Parra, M. Botella-Campos, J. Lloret and P. V. Mauri, “New Sensor Based on Magnetic Fields for Monitoring the Concentration of Organic Fertilisers in Fertigation Systems” Applied Sciences, vol. 10, no 20, pp. 7222, October 2020, doi: https://doi.org/10.3390/app10207222.

[14] Farnell.[Online]. Available from: h https://es.farnell.com/tektronix/afg1022/generador-se-al-2-can-func-arb/dp/2469113_ . [retrieved:April, 2021]

 ISBN: 978-1-61208-863-1